Study of interstellar extinction and circumstellar dust properties with composite porous grains

Ranjan Gupta

Inter University Center for Astronomy and Astrophysics

Pune-411007, India

Abstract

Its is well known that the interstellar dust plays the most important role in which the light seen form stars suffers extinction. Conventional models assume Mie theory of light scattering with solid spheres and other shapes of silicate and graphite particles of different sizes. An extension of this theory was Effective Medium Theory (EMT) which tries to explain some of the observed interstellar properties.

Abstract ... contd.

Recent space probes have confirmed that the dust grains are highly porous and fluffy (i.e. aggregates or clusters) rather than having regular shapes (spherical,cylindrical or spheroidal) and homogeneous in composition and structure. Since their is no exact theory for calculation of scattering properties of such irregular, inhomogeneous particles, recently our group has used Discrete dipole approximation (DDA) method and the results of this investigation will be discussed. The model uses a composite fluffy dust grain for explaining most of the observed interstellar extinction curves

Abstract ... contd.

Further, our composite dust model also explains the IR emission from circumstellar dust.

In the near future, there are a few space missions planned by ISRO and ESA viz. ASTROSAT and GAIA which will provide extensive platform for large coverage of UV sky and render interstellar extinction measurements where above models will be useful.

Plan Of The Talk

- Images of effects of dust and its composition
- Light Scattering Basics
- Scattering properties of composite grains and interstellar extinction – REAL DUST in Astrophysical Context
- Linear polarization calculations
- Abundance constraints
- IR emission from dust
- Laboratory Studies
- Future outlook

Dust in Astrophysical & Atmospheric Environments

Dust is a very important constituent in many astrophysical environments – though at most situations, its only 1% of the total mass in the ISM! Despite the fact that dust grains have relatively small contribution to the total mass, the remarkable efficiency with which such grains scatter, absorb, polarize and re-radiate the starlight – ensures that they have significant impact on our views of the universe.

Pillars of Dust

Nebula shows evaporating gaseous globules (EGGs) emerging from pillars of molecular hydrogen gas and dust

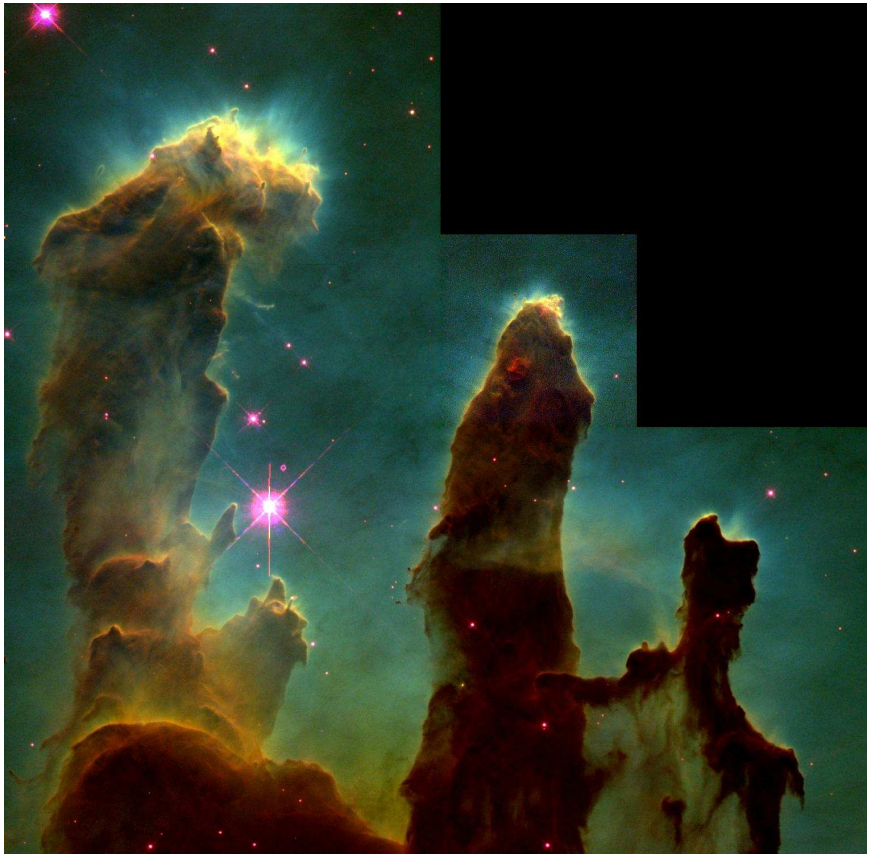

Bernard 68 Dark Cloud

The dependence of dust extinction at different wavelengths (B,V,I,J,H & K bands) for a dark cloud – background stars are seen more easily in longer wavelengths

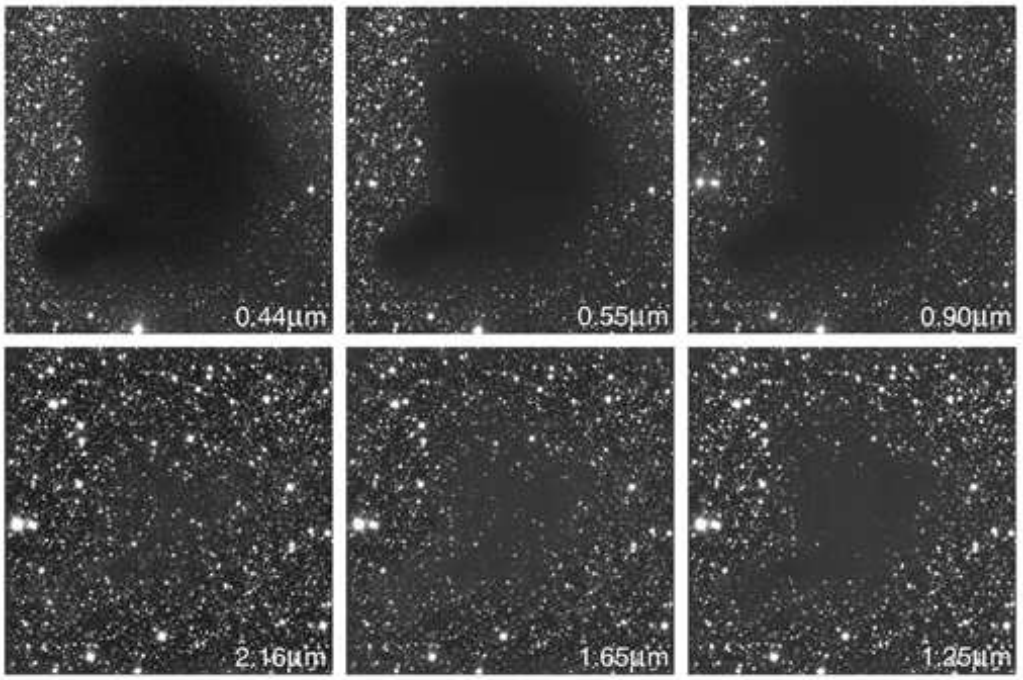

The Dark Cloud B68 at Different Wavelengths (NTT + SOFI)

ESO PR Photo 29b/99 (2 July 1999)

© European Southern Observatory

Rosette Nebula

Inside the Rosette nebula lies an open cluster of bright young stars designated NGC 2244. These stars formed about four million years ago from the nebular material and their stellar winds are clearing a hole in the nebula's center, insulated by a layer of dust and hot gas

Star forming cloud

The bright central source of heavily reddened star formation complex W3, which is completely invisible at visual wavelengths due to heavy dust obscuration, is one of the brightest stars in the Galaxy

Trifid Nebula

Clouds of glowing gas mingle with lanes of dark dust in the Trifid Nebula, a star forming region towards the constellation of Sagittarius. In the center, the three huge dark dust lanes that give the Trifid its name all come together

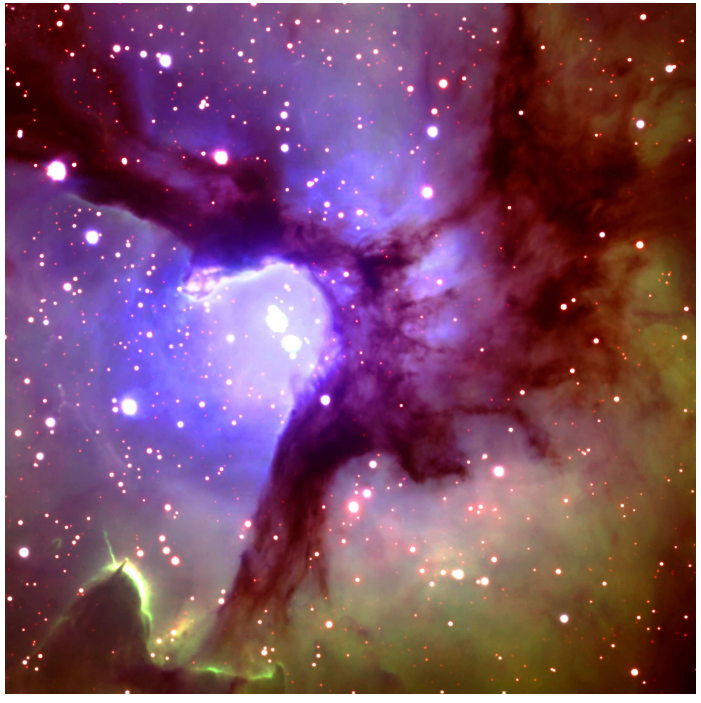

Horse Head Nebula

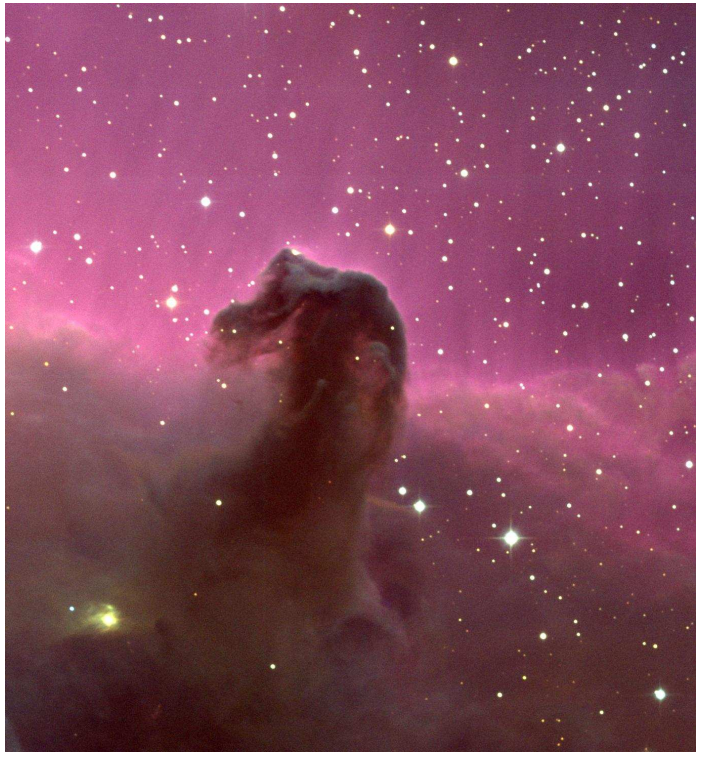

The Horsehead is a plume of dust rising in front of a background of glowing ionized gas off in one part of the Orion Molecular Cloud complex

Atmospheric Dust

Atmospheric dust effect seen during an eclipse

Views of a typical Sunset

Dust and its effect seen during a typical sunset

Dust Storm Onset

Onset of a dust storm – funnel like structure seen on a typical hot summer day

Sahara Dust Storm

An approaching major dust storm to be followed by a thunder storm and possible rain

Volcanic Dust

Another source of natural dust – may persist for many weeks – spread all over the globe by winds

Global Warming

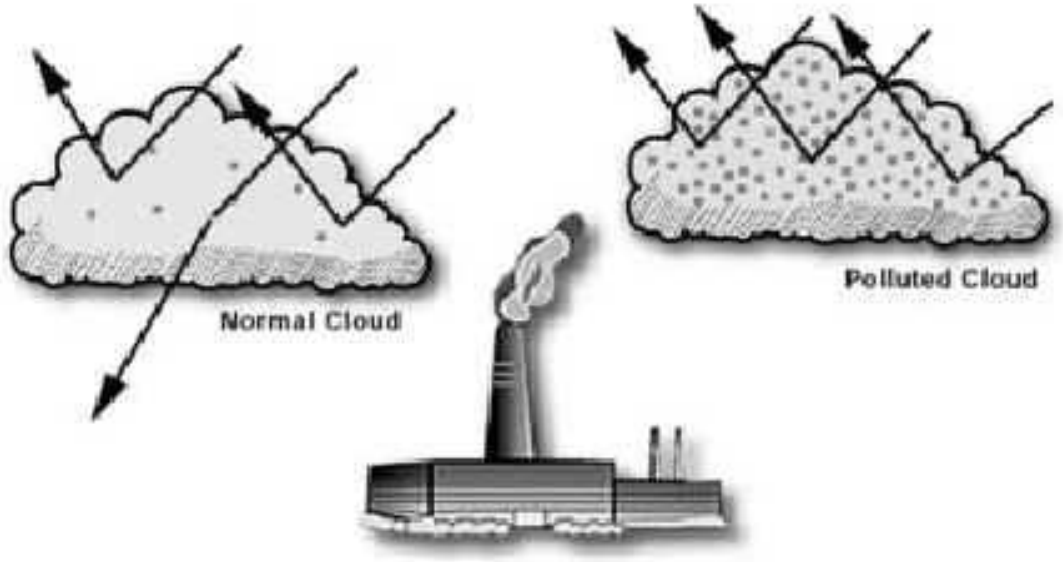

Figure 4. Clouds polluted by aerosols from factories have more numerous and smaller drops, causing the cloud to become brighter and reflect more of the Sun's radiative energy.

Source of man-made dust and its effect on global warming

Role of Dust

The main role of dust is to obscure the light from the background source which could be starlight or other general nebulosity. Dust causes the extinction of the background light; affects the polarization and also provides abundance contraints.

All the three aspects:

(1) Extinction

(2) Polarization

(3) Abundance contraints

have been studied in the past decade by our group.

Further recently, we have used composite silicate grains to explain the IR emission from circumstellar dust.

Light Scattering Basics

- Average total extinction = A_v = 1 magnitude kpc^{-1}
- Dust particles radius = a $\sim \lambda$
- Extinction Law $\propto \lambda^{-1}$
- Extinction Cross-section = $C_{ext} = Q_{ext} \pi a^2$
- Extinction Efficiency = $Q_{ext} = Q_{sca} + Q_{abs}$ (depends on 2 $\pi a/\lambda$ & m = n - ik)
- Density of Dust = $\rho \sim 1.2 \times 10^{-23}$ kg m^{-3}
- Gas to Dust Ratio = $\rho(\mathrm{dustparticles})/\rho(\mathrm{gas}) \sim 10^{-2}$

Light Scattering Basics .. contd.

- Number density per unit volume along the line of sight to a distant star = n_d
- Length of Cylinderical Column = L
- Number of Grains contained in a cylinderical column of length L and unit cross-section area = $N_d = n_d L$
- If instead of constant radius a, we have a size distribution

$$N_d = \int n(a) da$$

Light Scattering Basics .. contd.

- Number of Dust grains per unit volume having radius in the range of a and a+da = n(a)da
  $\propto \mathrm{a}^{-3.5}\mathrm{da}$
  (Mathis et.al. 1977 – power law grain size distribution – MRN Law)
- Total Extinction =
  $\mathrm{A}_\lambda = 1.086\mathrm{N}_\mathrm{d}\mathrm{C}_\mathrm{ext} = 1.086\mathrm{N}_\mathrm{d}\pi\mathrm{a}^2\mathrm{Q}_\mathrm{ext}$
  $= 1.086\pi \int \mathrm{a}^2\mathrm{Q}_\mathrm{ext}\mathrm{n}(\mathrm{a})\mathrm{da}$
  $= \pi \int_{\mathrm{a1}}^{\mathrm{a2}} \mathrm{a}^2\mathrm{Q}_\mathrm{ext}\mathrm{a}^{-3.5}\mathrm{da}$

References on Dust Modeling by our group

- Vaidya & Gupta, A & A, 328, 634 (1997)
- Vaidya & Gupta, A & A, 348, 594 (1999)
- Vaidya, Gupta, Dobbie & Chylek, 375, 584 (2001)
- Gupta, Mukai, Vaidya, Sen & Okada, A & A, 441, 555 (2005)
- Gupta, Vaidya, Dobbie & Chylek, Astrophys. Sp. Sci., 301, 21 (2006)
- Vaidya, Gupta & Snow, MNRAS, 371, 791 (2007)
- Vaidya & Gupta, JQSRT, 110, 1726 (2009)
- Roy, Sharma & Gupta, JQSRT, 110, 1733 (2009)
- Roy, Sharma & Gupta, JQSRT, 111, 795 (2010)
- Vaidya & Gupta, A&A, 528, 457 (2011)

Solid Spheres v/s Solid Spheroids

Extinction efficiencies $\mathrm{Q_{ext}(spheroid)/Q_{ext}(sphere)}$ v/s Wavelength for different grain sizes and axial ratios for Silicate and Graphite grains with T-Matrix.
Oblates have axial ratios $>$ 1.0 and Prolates have axial ratios $<$ 1.0 and sphere has axial ratio=1.0

Gupta et al., A&A, 441, 555 (2005)

Silicate Spheroids

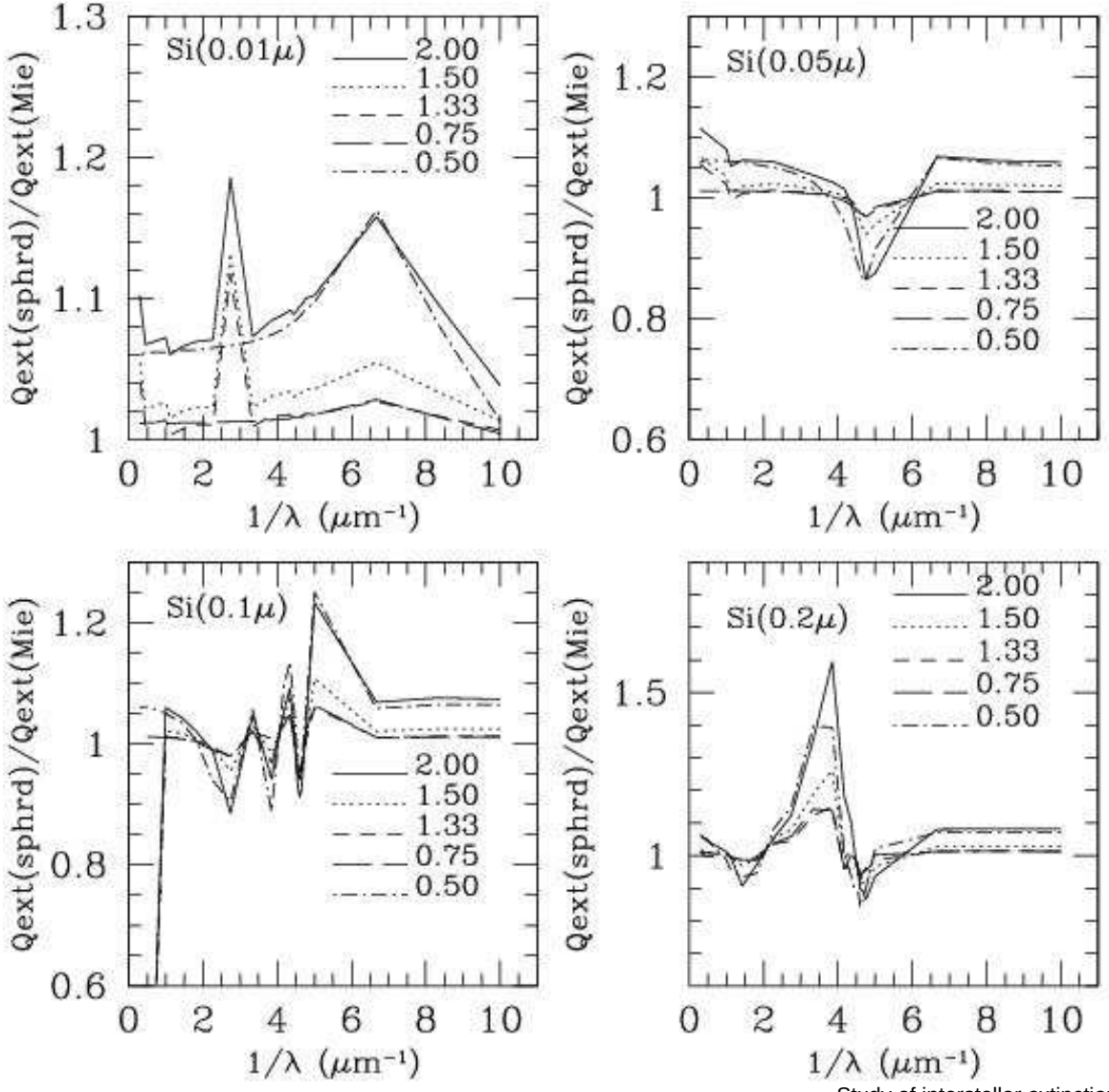

Graphite Spheroids

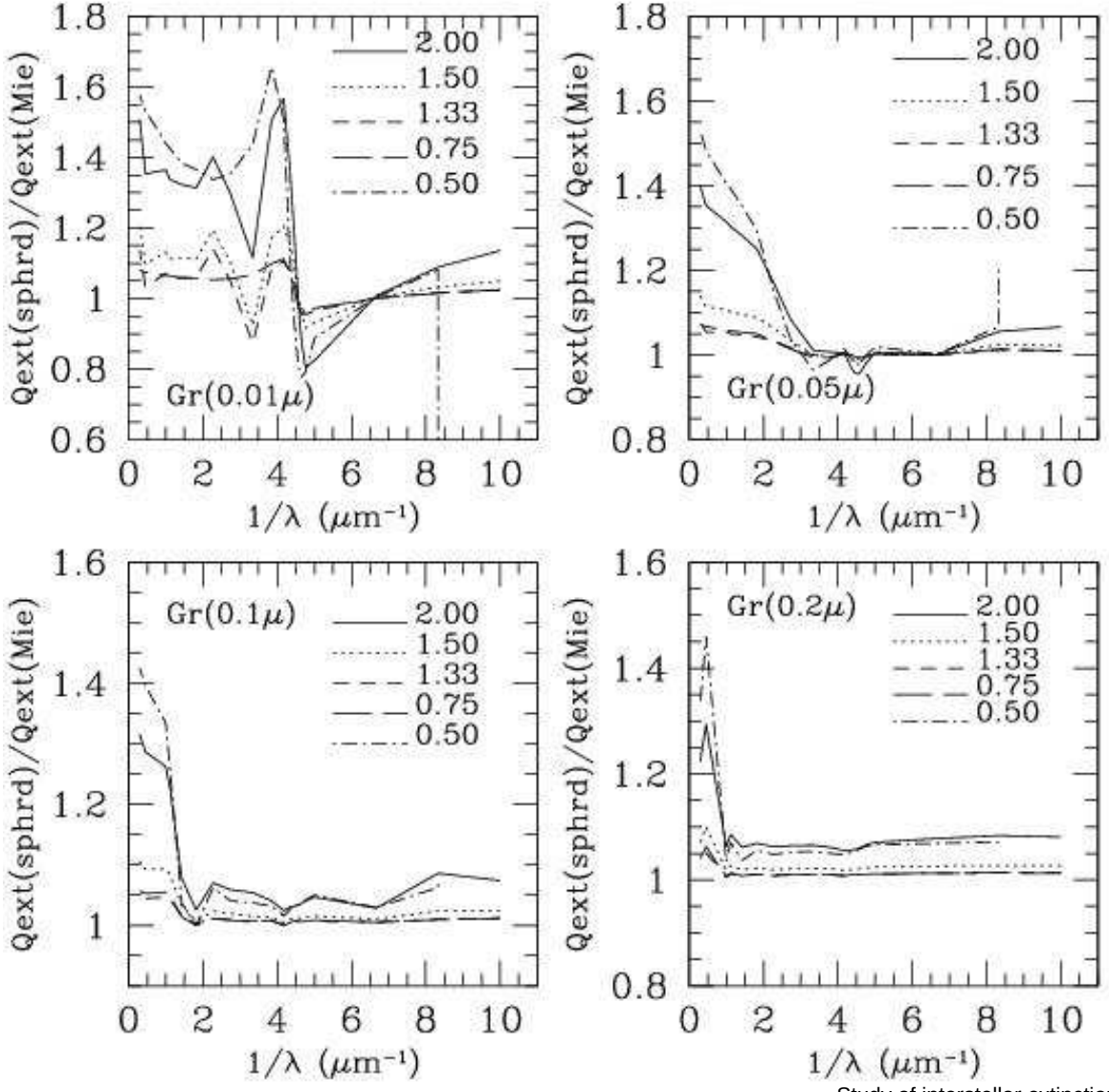

Graphite Bump Region

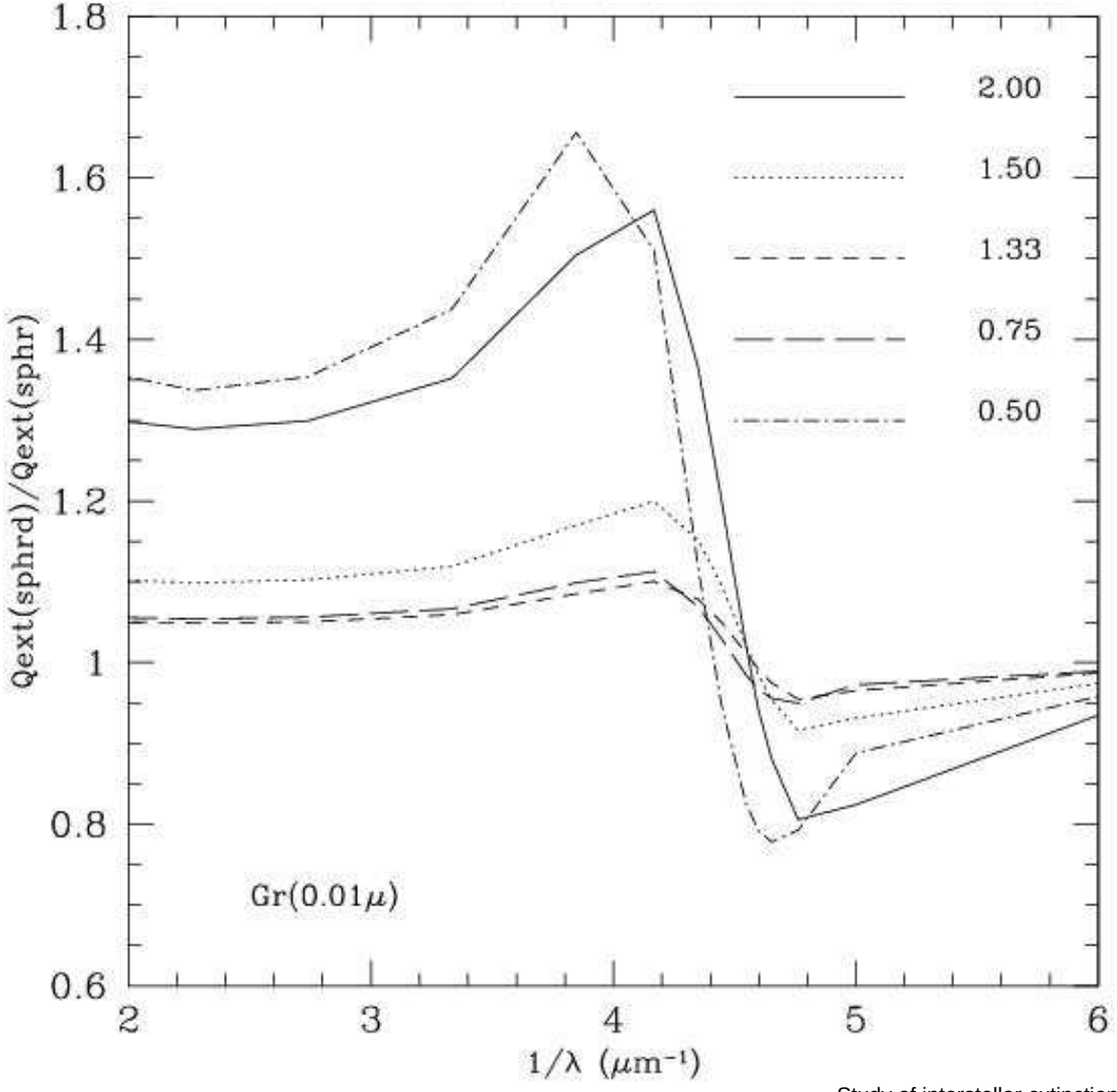

Interstellar Extinction Curves (Solid grains)

Comparison of Observed Interstellar Extinction curves with the best fit model combination curves of spheroidal silicate and graphite grains with various axial ratios using T-Matrix

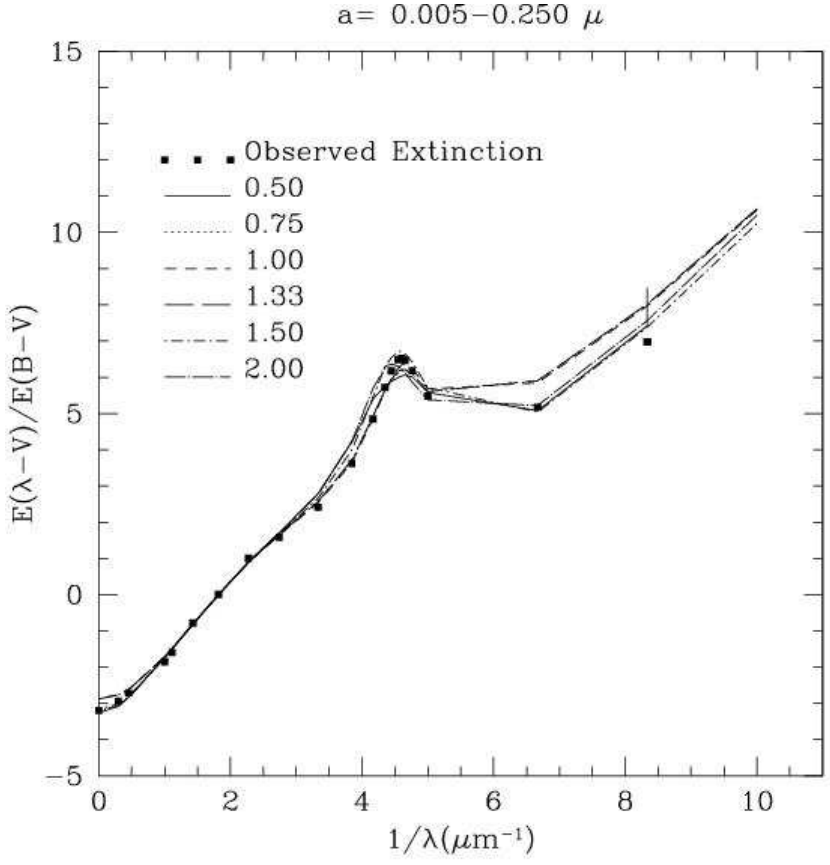

Int. Ext. Curve .. contd.

Bump Region

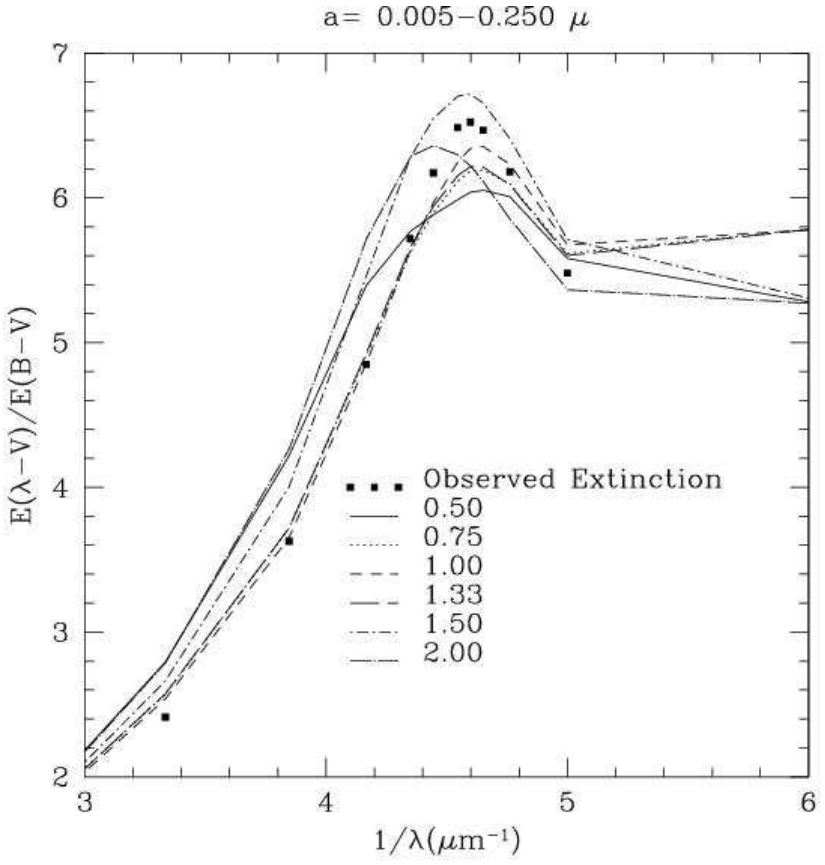

Extinction and linear polarization (Solid Grains)

Interstellar Extinction ($\mathrm{Q_{ext}}$) and Linear Polarization ($\mathrm{Q_{pol}}$) for aligned oblate spheroids (silicates and graphites) with grain size a=0.1μ. Various axial ratios (AR) and orientation angles of alignments have been computed.

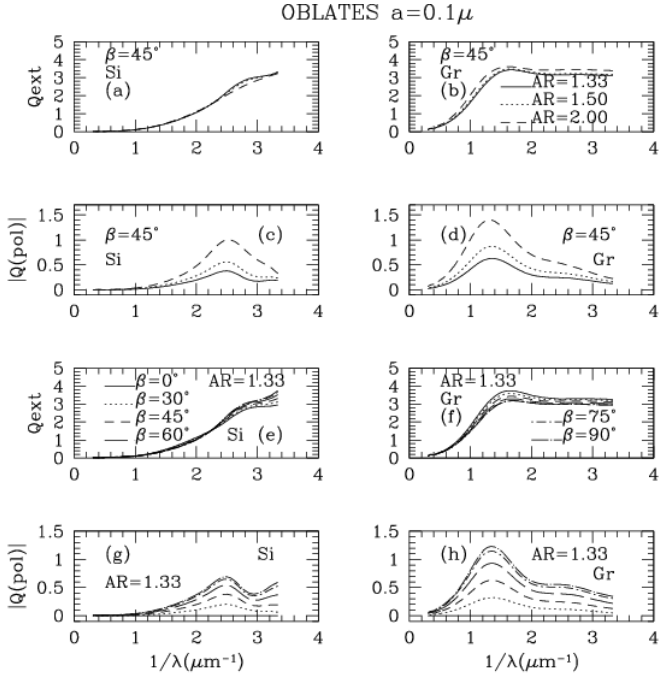

T-Matrix computations .. contd.

Interstellar Extinction ($\mathrm{Q_{ext}}$) and Linear Polarization ($\mathrm{Q_{pol}}$) for aligned prolate spheroids (silicates and graphites) with grain size a=0.1μ. Various axial ratios (AR) and orientation angles of alignments have been computed.

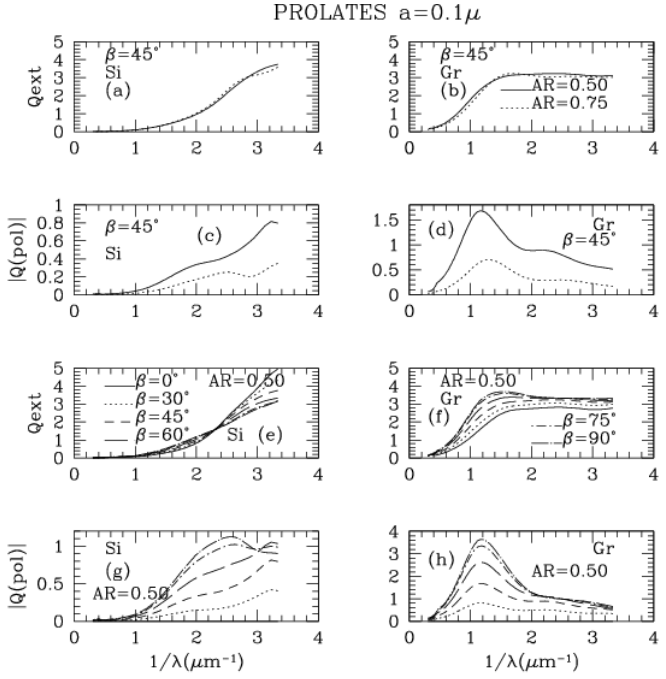

Observed Interstellar Extinction Curve

Observed Interstellar Extinction is compared with the best fit model curve of a combination of silicate and graphite grains with axial ratio AR=1.33 using a grain size distribution of 0.005-0.250μ in steps of 0.005μ. Lower panel highlights the UV bump region.

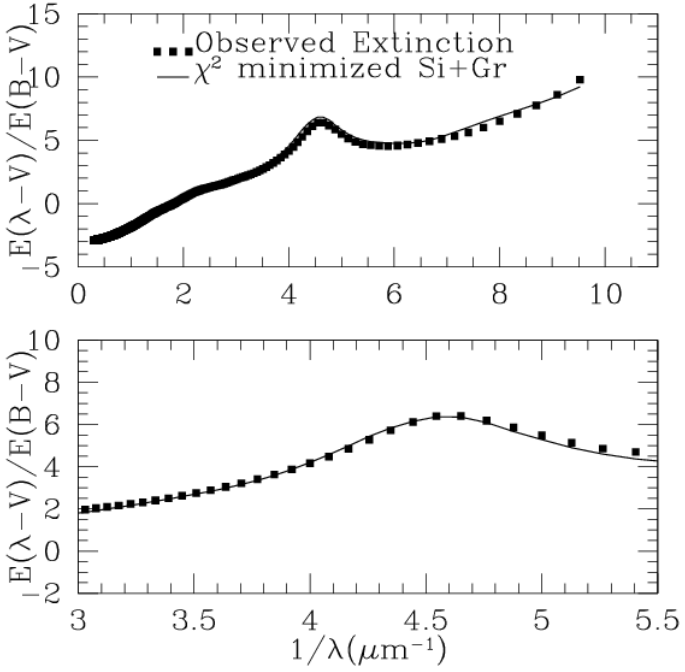

EMA & T-Matrix

Fitting of Observed Extinction curve with Effective Medium Approximation (Maxwell-Garnet mixing rule) and T-Matrix computation

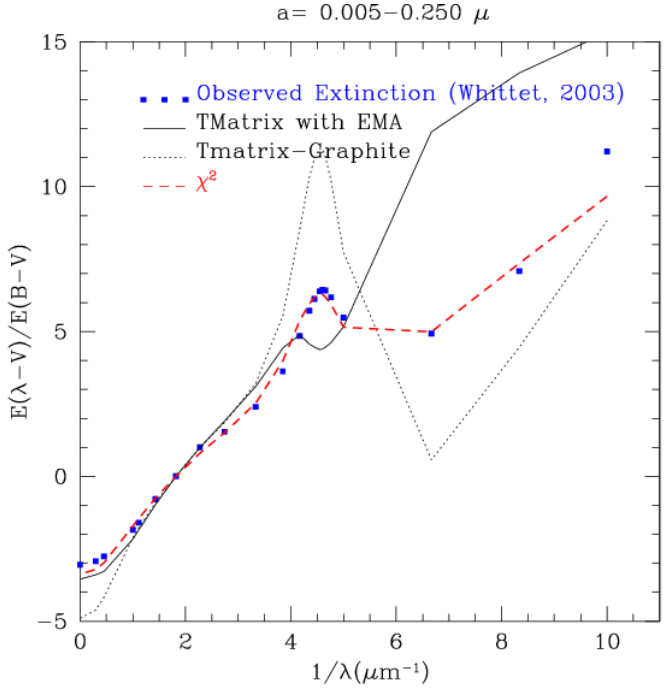

Discrete-Dipole Approximation (DDA) Basics

Computation for solid spheres which are homogeneous and isotropic (cylinders and some more shapes are also possible) could be done by Mie scattering theory. It is clear that dust grains cannot be solid spheres or of same composition since observation of interstellar and other polarization requires non-spherical grains. T-Matrix and some other exact methods can be used to model non-spherical grains but usually of single composition.

DDA for computing light scattering of particles – originally developed by Purcell & Pennypacker (1973) can handle non-spherical grains. DDA replaces the solid grain by an array of N point dipoles, with the spacing between the dipoles small compared to the wavelength. Each dipole has an oscillating polarization in response to BOTH an incident plane wave and the electric fields due to all of the other dipoles in the array (see Draine, ApJ, 333, p848-872, 1988 for more details on DDA method).

"Spherical" Dipole Arrays

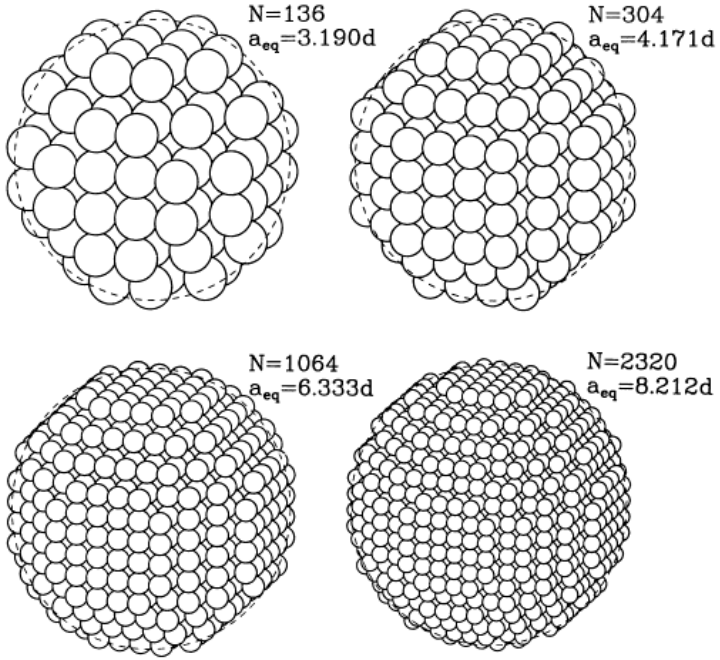

FIG. 1.—"Spherical" discrete dipole arrays considered in this paper, with $N = 136, 304, 1064$, and 2320

approximately as $N^{-1/3}$, consistent with the error being associated with the granularity of the surface. On the basis of a limited number of numerical calculations for spheres, we estimate that in order to attain a fractional error less than Δ (in the zero-frequency limit) the particle should satisfy the criterion

$$N > N_{\rm min} \approx 60\,|m-1|^3(\Delta/0.1)^{-3}\,. \qquad (4.01)$$

This estimate for $N_{\rm min}$ applies to spheres; $N_{\rm min}$ for other convex shapes will differ by factors of order unity. The strong dependence on $|m-1|$ implies that discrete dipole calculations for materials with large refractive indices must either accept relatively large fractional errors Δ, or else employ very large values of N.

b) Granularity versus Wavelength and Skin Depth

A second necessary condition for the dipole array to provide an accurate representation of a homogeneous grain is that the length scale for variation of the electric field within the grain must be large compared to d. For specified $ka_{\rm eq}$ and refractive

not just compared to the wavelength *in vacuo* $2\pi/k$ but also with the wavelength $2\pi/{\rm Re}(m)k$ within the material. In the event that the material is absorptive, a second necessary condition is that d be small compared to the attenuation length (or "skin depth") $2\pi/{\rm Im}(m)k$ for the electromagnetic wave. A simple criterion suggests itself: $kd\,|m| < \beta$, where β is some constant of order unity; obviously the value of β will depend on the desired degree of accuracy. Based on our calculations for $m = 1.7 + 0.1i$ (see § VI) we estimate the dimensionless factor $\beta \approx 1.0(\Delta/0.1)$, where Δ is the desired fractional accuracy. One thus obtains a condition on N:

$$N \gtrsim \frac{4\pi}{3}\,(ka_{\rm eq})^3\,|m|^3\left(\frac{\Delta}{0.1}\right)^{-3}\,. \qquad (4.02)$$

As expected, large values of N will be required to compute scattering for large values of $ka_{\rm eq}$, or for materials (such as conductors) with large values of $|m|$.

Dipole Polarization within the "Spherical" Arrays

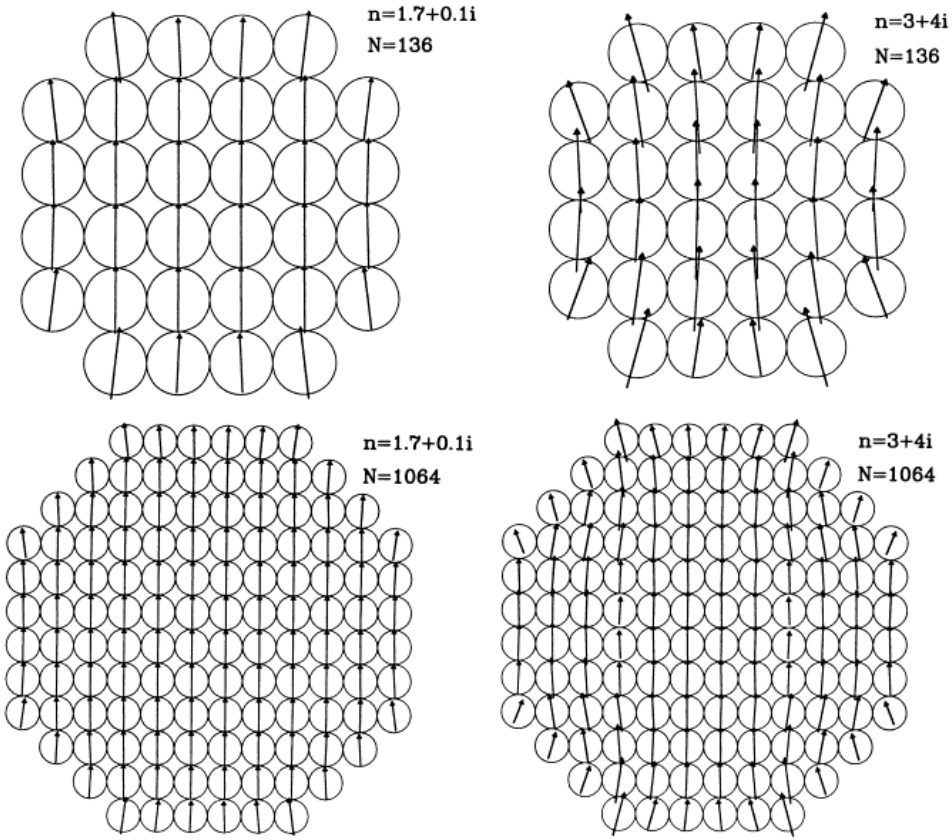

FIG. 2.—Dipole polarizations within "spheres" consisting of $N = 136$ and $N = 1064$ dipoles, in a static uniform applied electric field. The applied electric field is in the y-direction; shown are the dipoles lying on the $z = d/2$ plane. The four cases are labeled by the number N of dipoles and the complex refractive index n. The individual polarization vectors would be parallel and of length equal to d if the polarization per dipole were equal to the polarization within a continuum sphere (see text). It is seen that significant departures from the continuum limit occur at "corners" along the sphere boundary; the fraction of the array elements located along the boundary decreases as $N^{-1/3}$. It is also seen that departures from the continuum limit are more pronounced for large values of the refractive index m. As discussed in the text, this surface "granularity" is a significant source of error for large values of the refractive index m; suppression of this error may require very large values of N.

(3.05). To estimate the relative importance of magnetic dipole absorption, consider a spherical volume, of radius $r = (3/4\pi)^{1/3}d$, having the same volume as our unit cell. For this sphere the ratio of magnetic dipole absorption to electric dipole absorption is (Draine and Lee 1984)

Evidently magnetic dipole effects are an important consideration when $|m| \gtrsim (36\pi)^{1/3}(\Delta/0.1)^{-1/2} = 4.83(\Delta/0.1)^{-1/2}$. For given N, the validity criterion (4.04) is equivalent to a limit on ka_{eq}:

Validity Criteria fo DDA

Grain volume V is represented by an array of N discrete dipoles – physical size of the grain is characterized by the "equivalent radius" $a_{eq} = (3V/4 * \pi)^{1/3}$ – i.e. radius of a sphere of equivalent volume. The nearest neighbour distance between the dipoles is $d = a_{eq} * (4 * \pi/3N)^{1/3}$

(a) The DDA is valid only when the N is large enough (d is small enough compared to the a_{eq}) such that the boundary of the cubic array satisfactorily approximates the desired grain shape.

(b) Another criteria is $|m|kd < 1$ – where m is the complex refractive index; k is π/λ and d is the lattice spacing.

Validity Criteria .. contd.

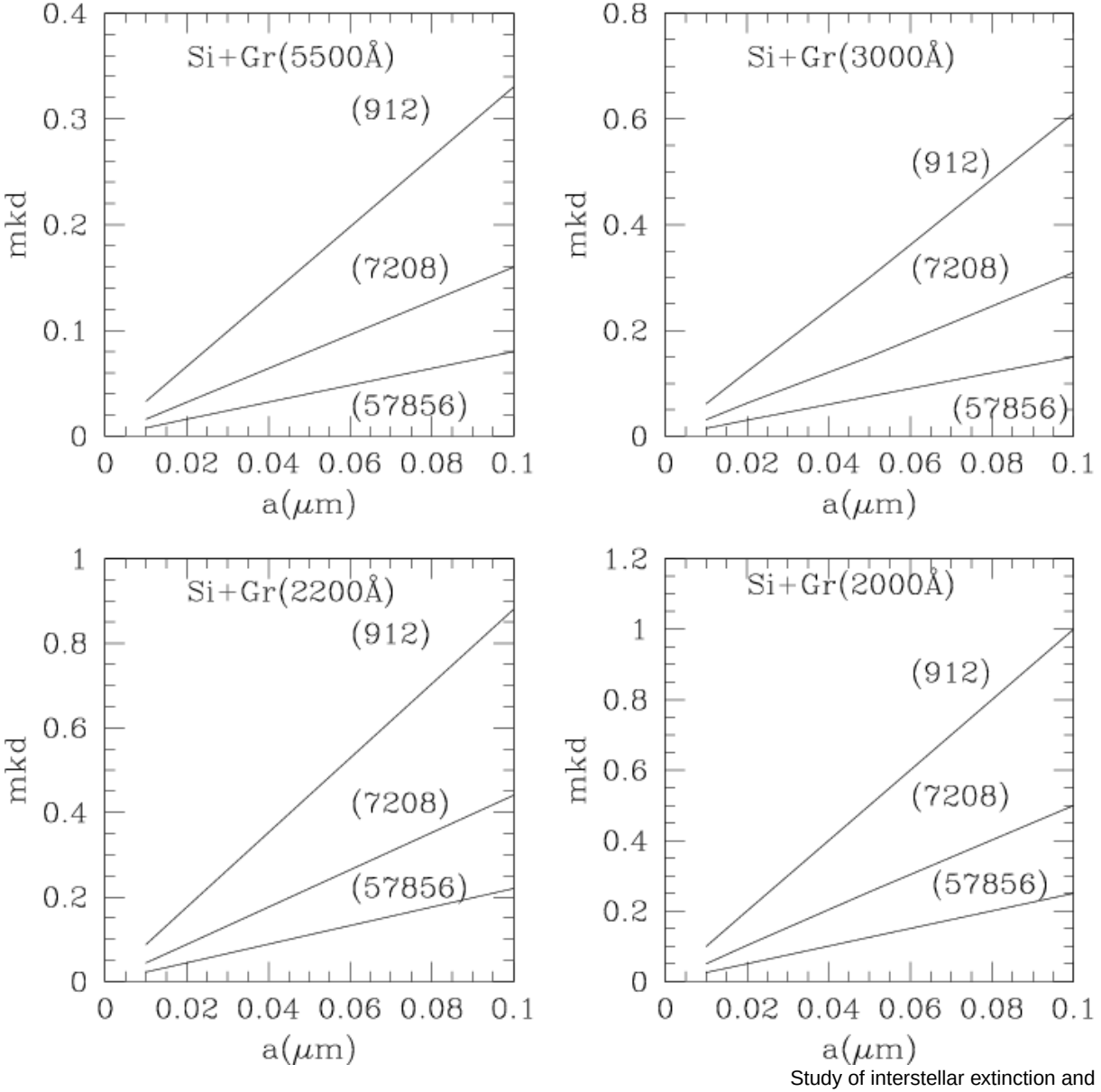

Validity Criteria .. contd.

Table 1: DDA validity criteria in Optical/UV

$\lambda\ (\mu m)$	N=9640	14440	25896
	a(μ)	a(μ)	a(μ)
3.4000	4.00	5.00	6.00
2.2000	2.50	3.50	4.00
1.0000	1.20	1.40	1.60
0.7000	0.80	1.20	1.00
0.5500	0.60	0.96	0.80
0.3000	0.40	0.50	0.45
0.2000	0.22	0.30	0.25
0.1500	0.14	0.20	0.16
0.1000	0.10	0.16	0.12

Validity Criteria in IR

Table 2: DDA validity criteria showing the $|\mathrm{m}|\mathrm{kd} \leq 1$ values for each model in IR region for maximum grain size of a=0.250μ.

$\lambda\ (\mu m)$	N=9640	14440	25896
5.0	0.041	0.030	0.022
10.0	0.021	0.014	0.011
15.0	0.015	0.011	0.005
20.0	0.011	0.007	0.003
25.0	0.005	0.002	0.001

Porosity

Porosity P is defined as:

$\mathrm{P} = 1 - \mathrm{V_{solid}}/\mathrm{V_{total}}$; where $\mathrm{V_{solid}}$ is the volume of the solid material inside the grain and $\mathrm{V_{total}}$ is the total volume of the grain. Porosity varies between $0 < \mathrm{P} < 1$

Axial Ratios & No. of Inclusion (no. of dipoles/inclusion)

Inclusions	Inclusion	Fractions	
N=9640	f=0.1	f=0.2	f=0.3
AR=1.33	32/24/24		
16/12/12	1(1184)	2(1184)	
8/6/6	6(152)	11(152)	16(152)
4/3/3	38(16)	76(16)	114(16)
N=25896	f=0.1	f=0.2	f=0.3
AR=1.50	48/32/32		
12/8/8	7(432)	13(432)	19(432)
6/4/4	54(56)	108(56)	162(56)
3/2/2	216(8)	432(8)	648(8)
N=14440	f=0.1	f=0.2	f=0.3
AR=2.00	48/24/24		
16/8/8	3(536)	6(536)	8(536)
12/6/6	6(224)	11(224)	16(224)
8/4/4	23(64)	46(64)	68(64)

Orientation Averaging

β from 0 to 180 degrees in 3 steps
θ from 0 to 90 degrees in 3 steps
ϕ from 0 to 180 degress in 3 steps

Total 27 orientations are good enough

Composite Grains

It is very unlikely that interstellar grains have regular shapes (spherical/cylinderical/spheroidal) or that they are homogeneous in compostion and structure. It has been proven that (from balloon observations and other flyby missions) the real dust grains are porous; fluffy and non-spherical – rather than solid spheres as was assumed in Mie theory for computation of light scattering properties by dust grains.

Composite Grains .. contd.

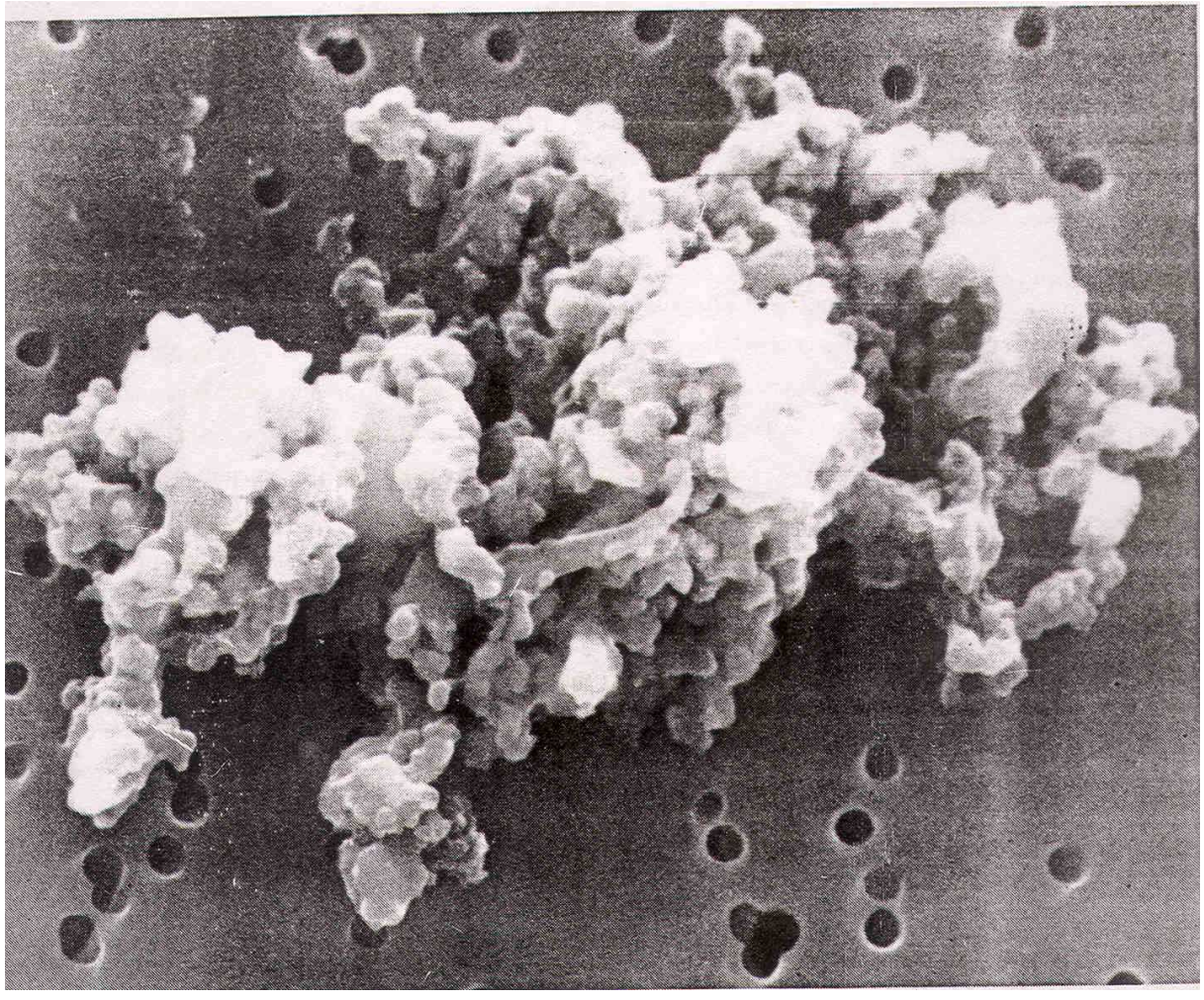

Composite Grains .. contd.

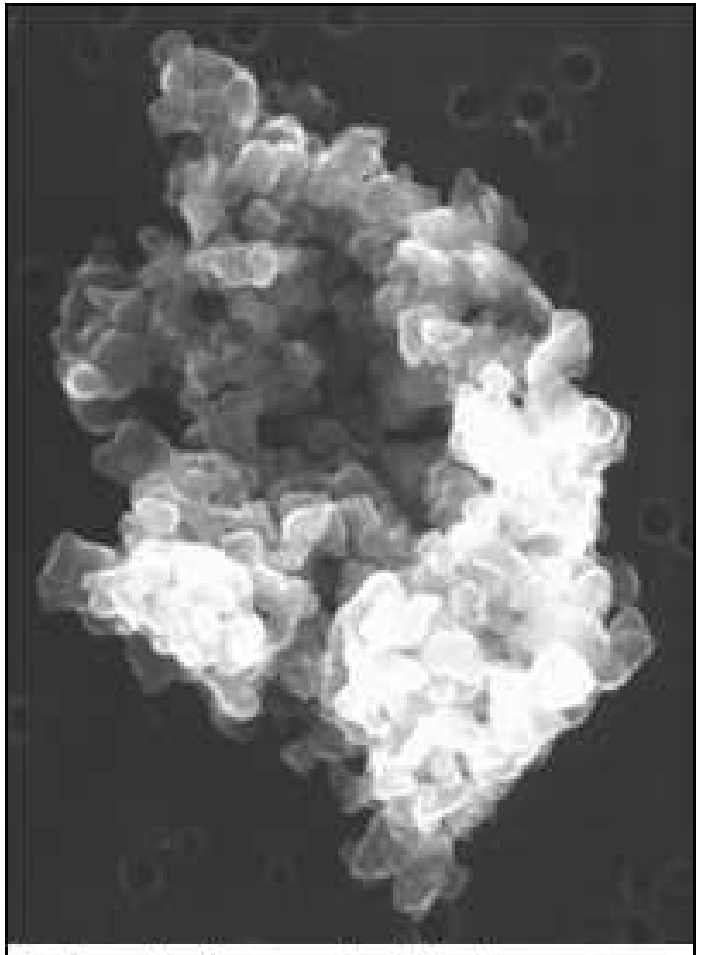

Cosmic dust grain 11 micrometers in diameter.

Composite Grains .. contd.

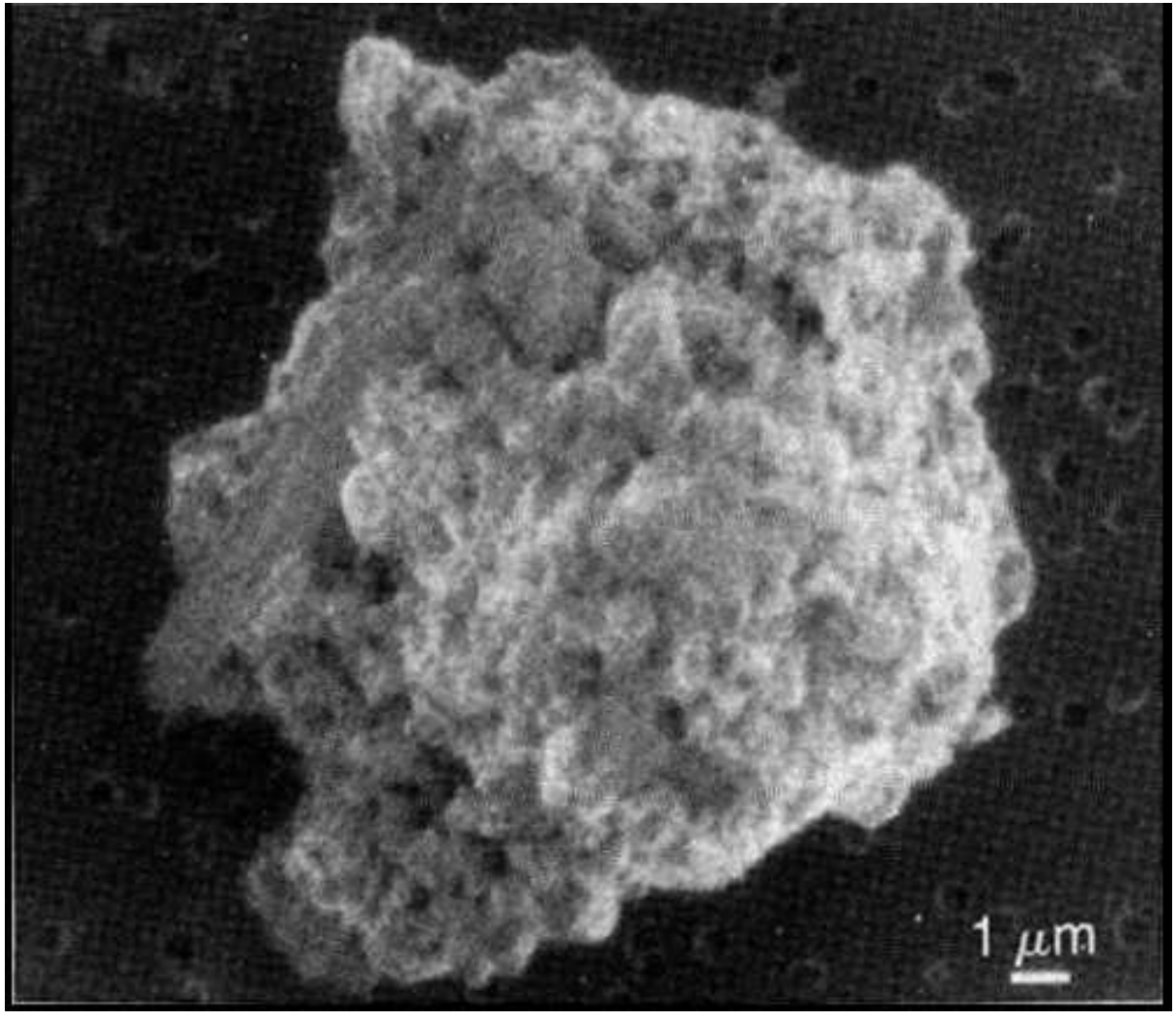

Composite Grains .. contd.

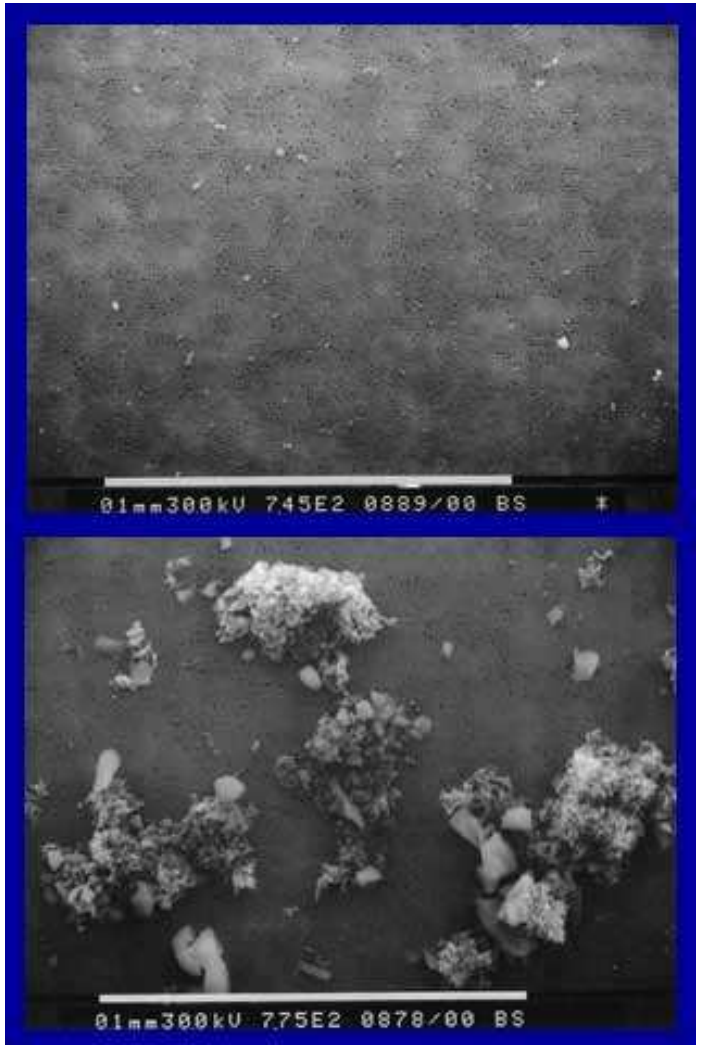

Aerogel Dust Tracks from Impact mission

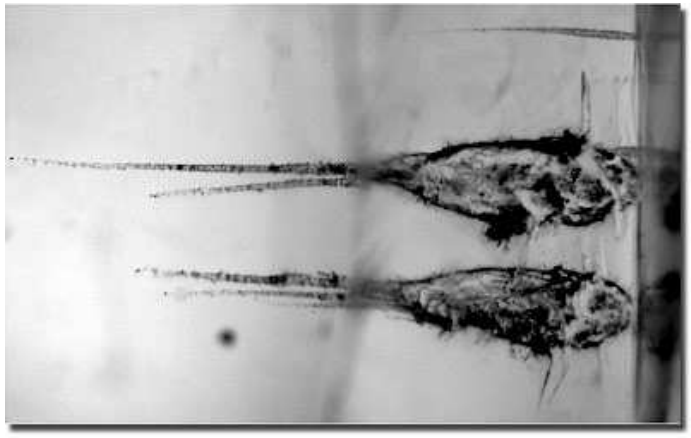

Simulated Grains

Multi-component-composite; size distribution and porous etc.

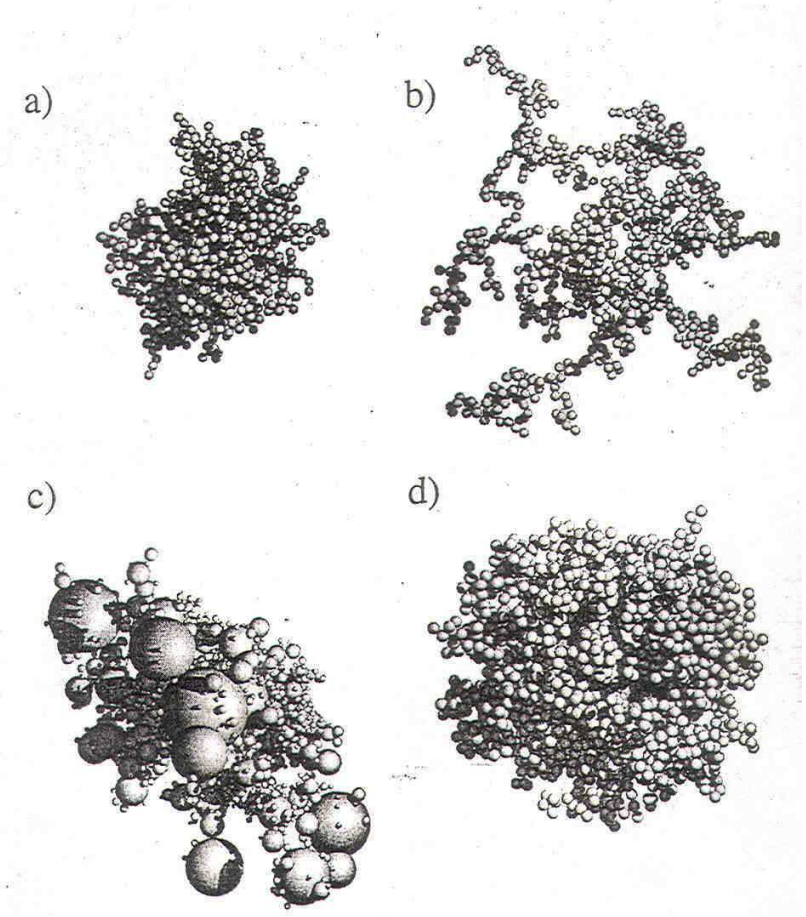

Figure 8.4. Computer simulations showing examples of particles formed by grain–grain coagulation (Dorschner and Henning 1995). (*a*) A compact particle produced by particle–cluster aggregation of 1024 identical small spheres. (*b*) A loose fractal particle produced by cluster–cluster aggregation of 1024 identical small spheres. (*c*) A composite particle produced by particle–cluster aggregation of 2001 spheres with sizes following

Simulated Grains .. contd.

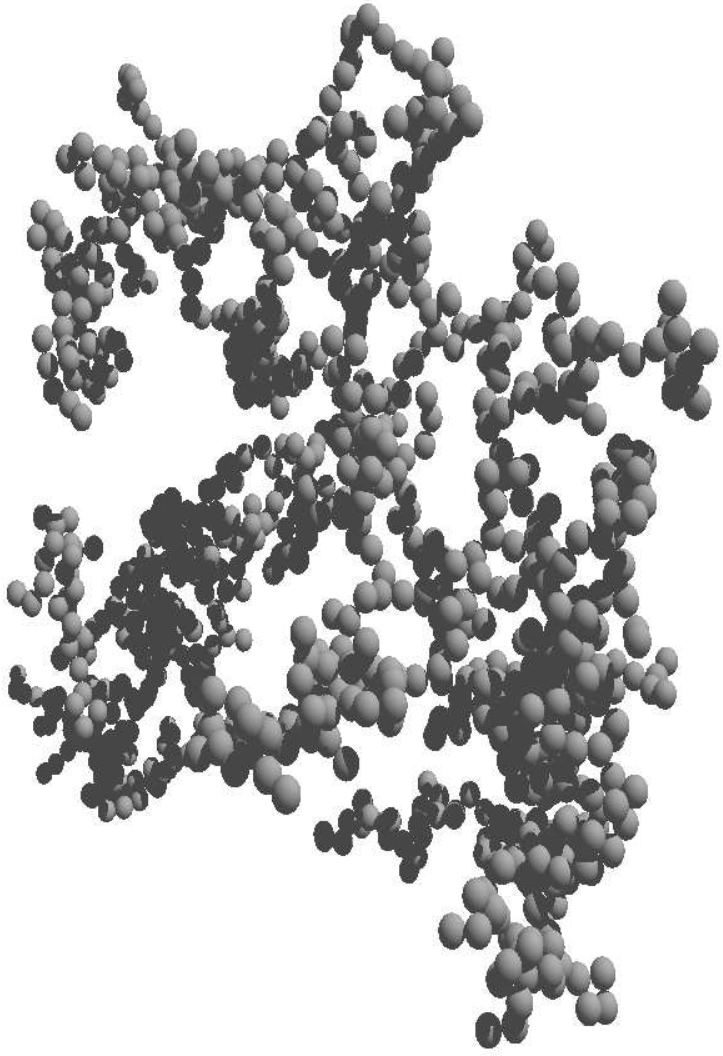

Composite Grains with Inclusions

A typical Non-spherical Composite grain with a total of N=9640 dipoles with the inclusions embedded in the host spheroid such that only the ones placed at outer periphery are seen. (Gupta et al., Astrophys. Space Sci., 301, 21 (2006))

Composite Grains with Inclusions .. contd.

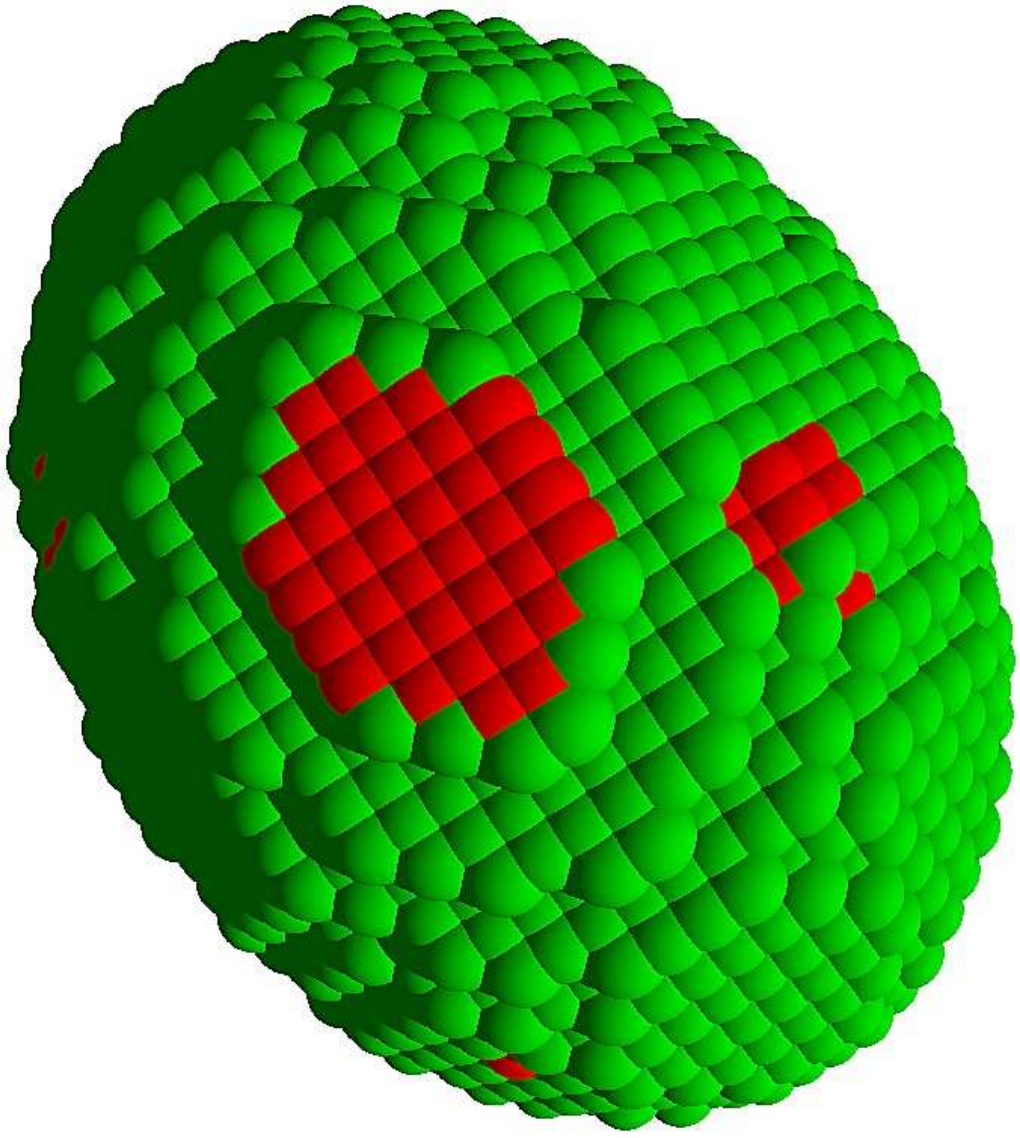

Showing the Inclusions

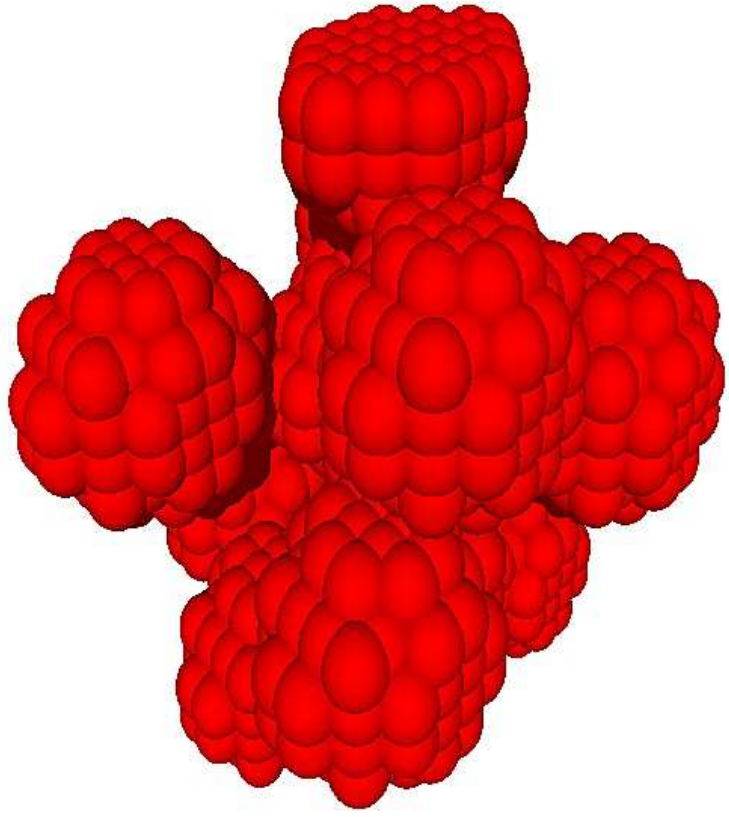

Interstellar Extinction with composite grains

Gupta et al., Astrophys. Space Sci., 301, 21 (2006)

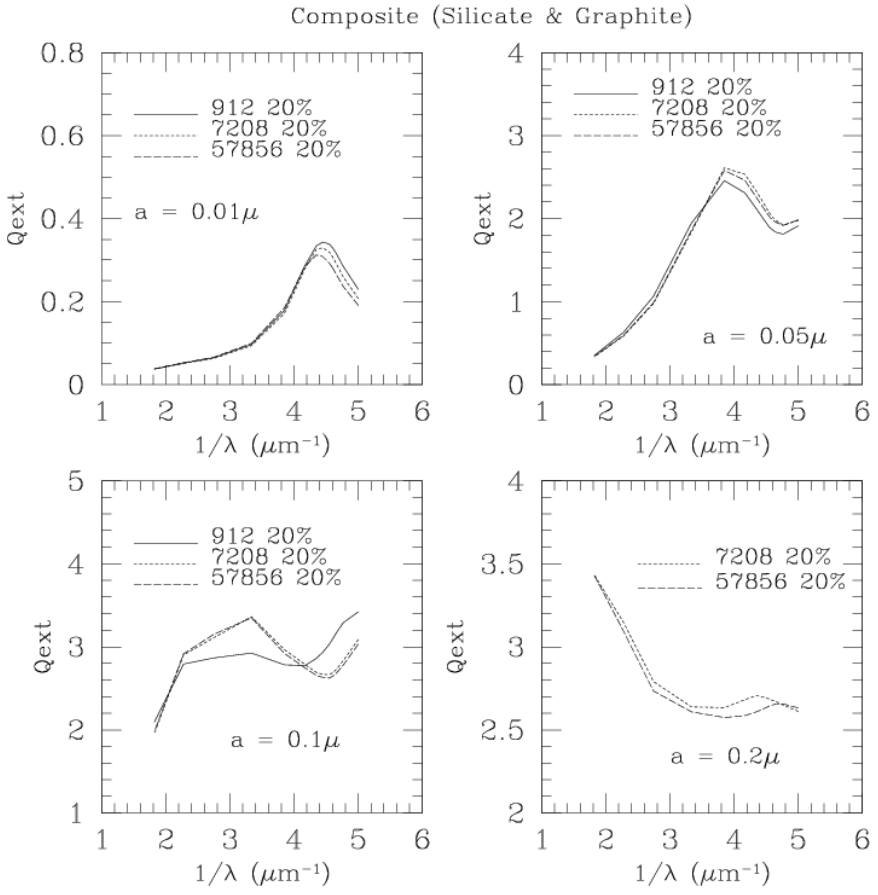

Int. Ext. .. contd.

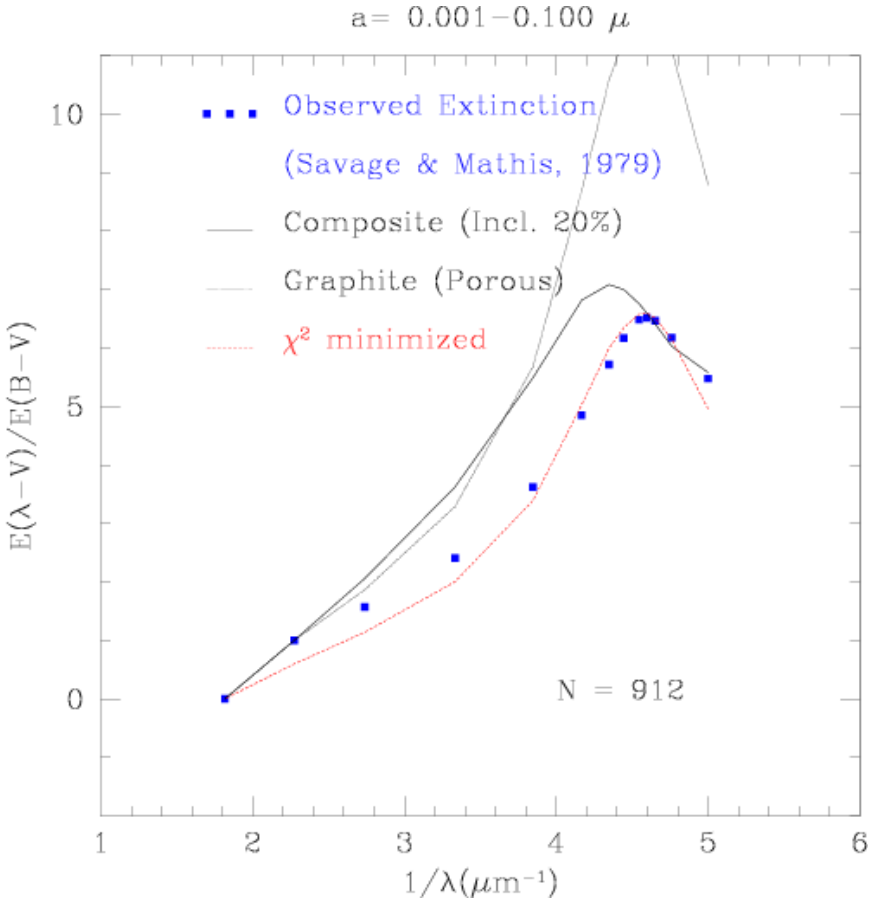

Cometary Polarization

3D plots of Scattered Intensity (S11) and Linear Polarization (P) for Composite Spheroidal Grains (N=14440 & 152) with silicate as host sphere and 20 % graphite as inclusion. The vertical axes are for S11 and P; the axes marked as θ denotes the Scattering angle (X 10°) in the range 0 to 180° and the third axis is for the grain size a=0.0-1.0μ. The wavelength for these calculations in the K-band at 2.2 μm.

Cometary Polarization .. contd.

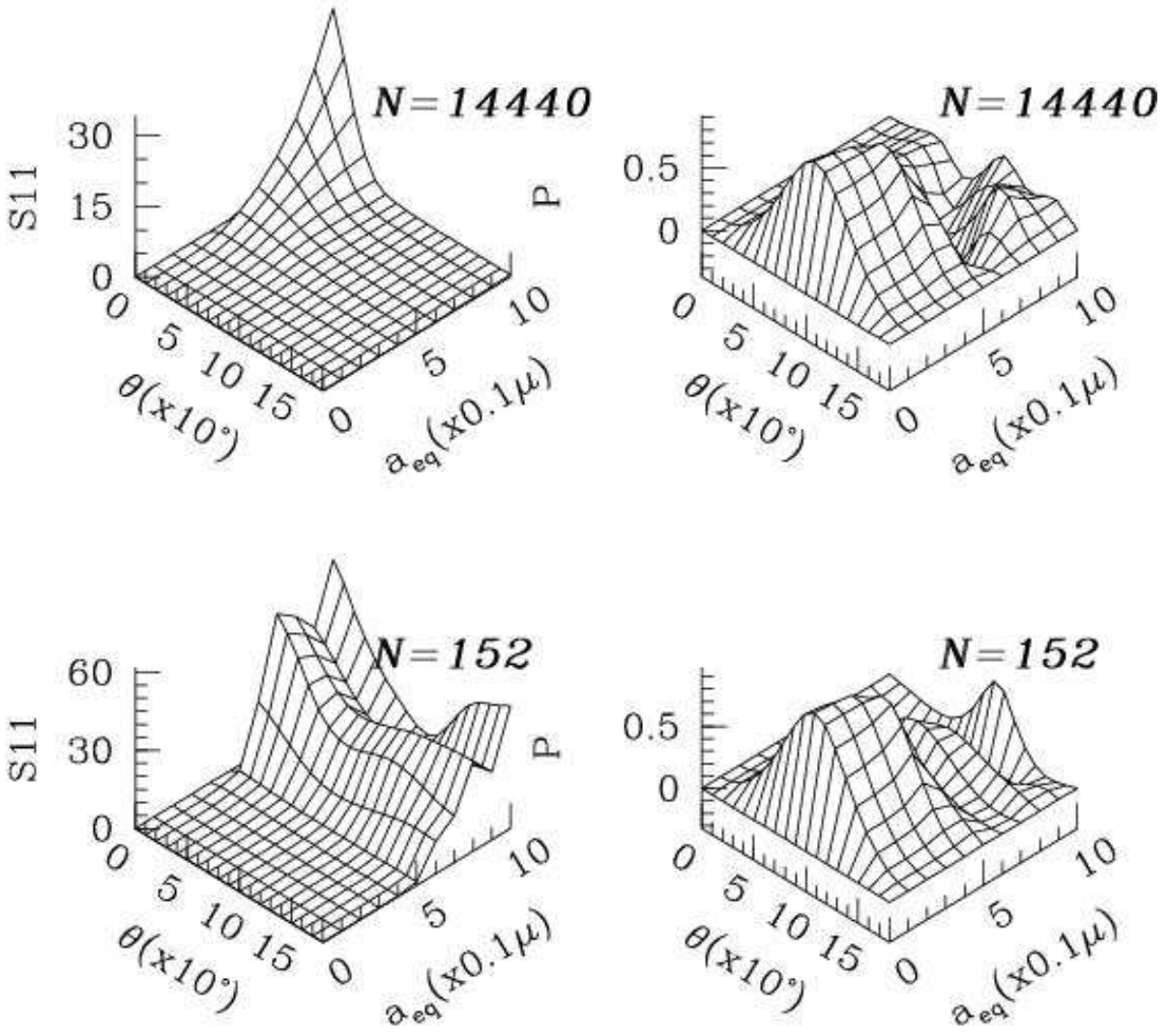

Cometary Polarization .. contd.

Linear Polarization (P) for Spheroidal Composite Grains (N=25896, 14440 and 152) with silicate as host sphere and graphite as inclusion and comparison with the observed Polarization data for comets

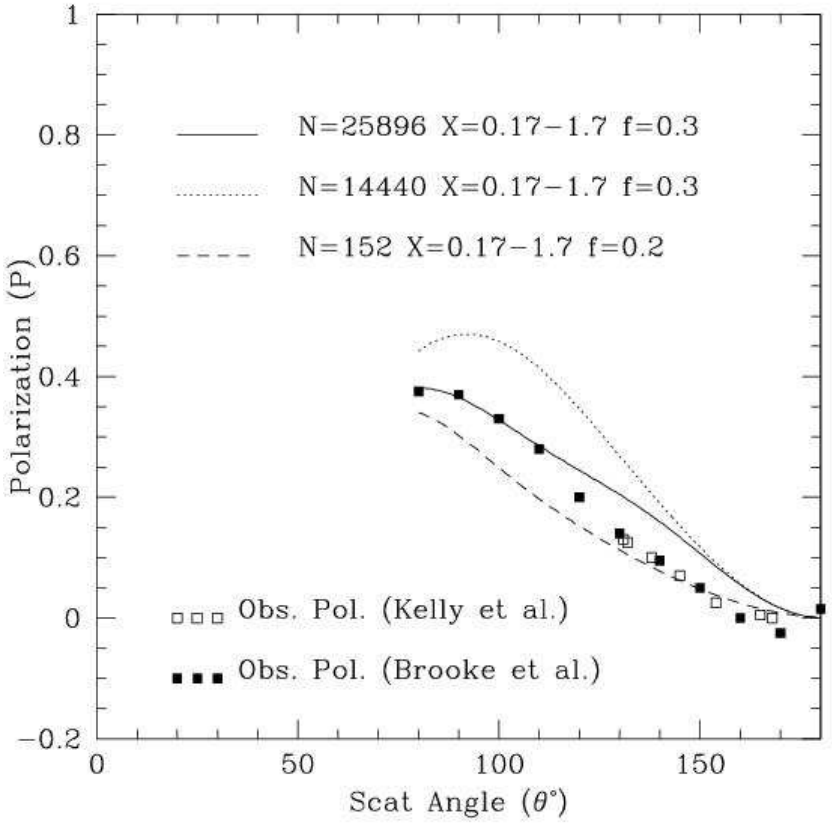

Cometary Polarization .. contd.

Note that some comets show the negative branch of polarization at large scattering angles (i.e. $> 150^{\circ}$) but not all comets show this negative branch in the K-band (Kelly et.al. 2004). Our models do not show this negative branch but the overall curves resemble well with the observations. Calculations are in progress for using fractal aggregate monomers as a model for dust grains which can reproduce the negative branch of polarization.

Interstellar Polarization by Composite Grains

Linear Polarization for N=9640 dipoles and two volume fractions (f=0.05 & 0.10) and comparison with Serkowski's Law (Vaidya et al. 2007, MNRAS, 371, 791)

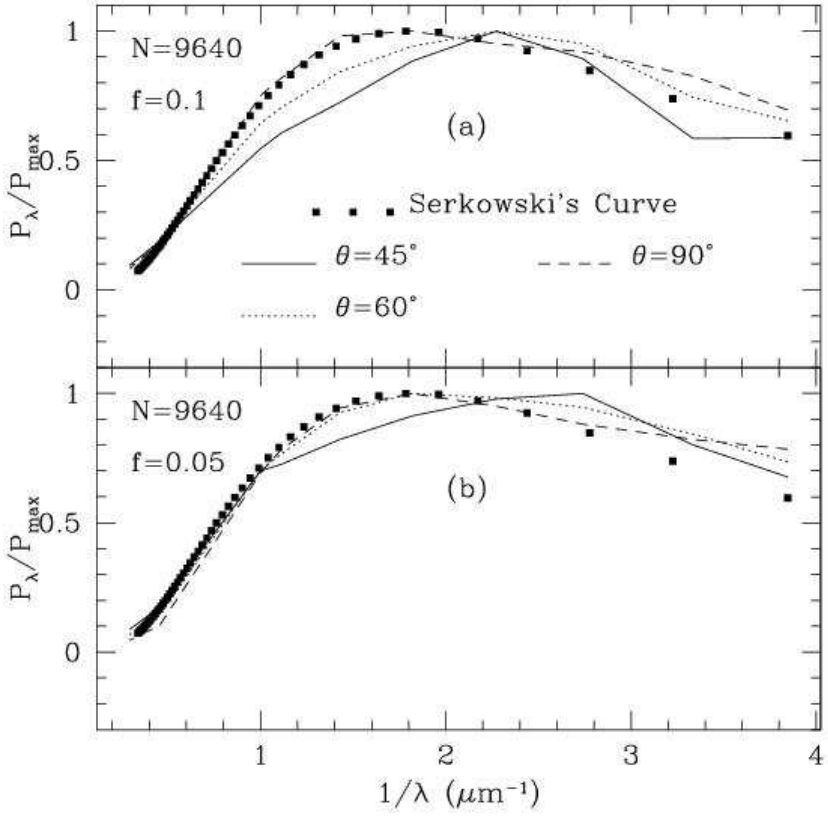

Abundance Constraints & Carbon Crisis

Table 3: Abundance Ratios

Abundance Ratio (ppm)	ISM	Other Models	Our Model
C/H	110	254	160
Si/H	17	32	25

ISM Value: Estimated by Mathis, JGR, 105, 10269 (2000)
Other Models: Li & Draine, ApJ, 554, 778 (2001)
Our Model (Vaidya et al. 2007, MNRAS, 371, 791)

Abundances .. contd.

Calculations with our models predict lower values for Carbon and Silicon abundances as compared to other composite models but a further reduction is warranted to match the estimated ISM values and this could be achieved by introducing a 3rd component in the composite grain like SiC, amorphous carbon and PAH's etc.

The calculations have been done by using the Volume Extinction Coefficient $\mathrm{V_c} = \sum \mathrm{V} / \sum \mathrm{C_{ext}}(\lambda)$ for obtaining the abundances for our models (spheres and spheroids) with various axial ratios and porosities etc.

Light Scattering Codes

- http://www.astro.spbu.ru/staff/staff/ilin2/SOFTWARE/
- http://www.astro.princeton.edu/∼draine/DDSCAT.html
- http://www.giss.nasa.gov/∼crmim/t_matrix.html

IR emission from circumstellar dust

Composite grain model has been used to compute IR fluxes in the 5-25μm region at several dust temperatures T=200-350°K and compared with the IRAS-LRS average observed curves and also for two other typical stars which are known to have strong Silicate emission features at 10 and 18 μm.

IR flux comparison with compos-ite models and observed fluxes

Best fit χ^2 minimized composite grain models (silicates with graphite inclusions) plotted with the average observed infrared flux for IRAS-LRS curve and two other stars (A&A, 528, 457, 2011)

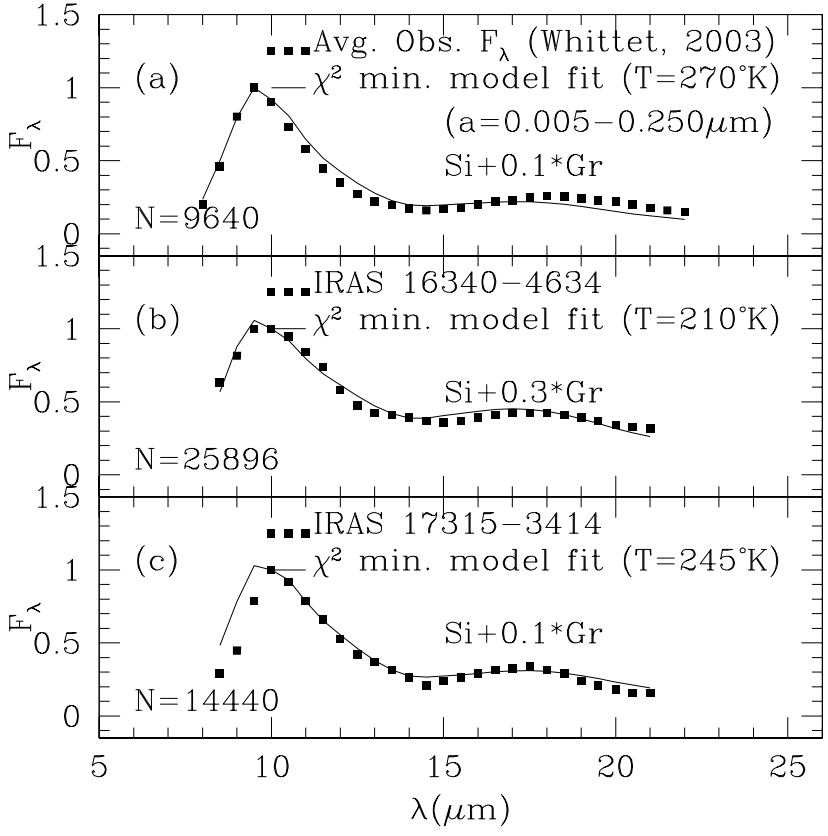

Analytical formulae for Interstellar Extinction

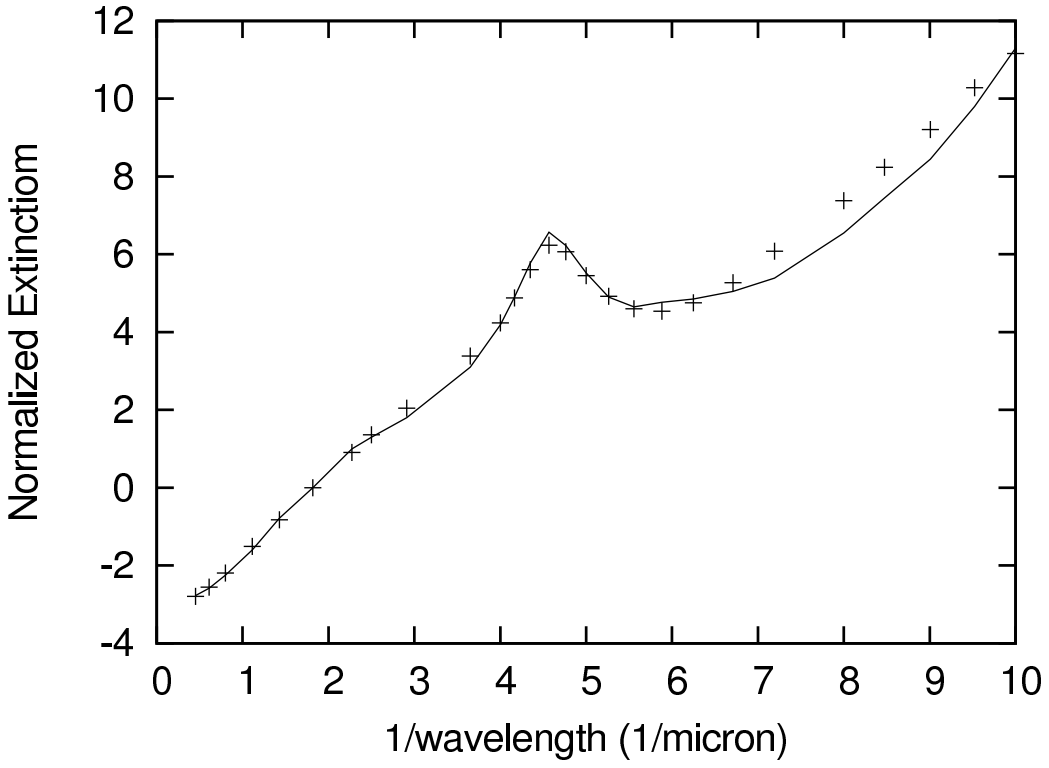

Figure 1: Analytical formulae fit to the observed averaged Extinction Curve – JQSRT, 111, 795 (2010)

Extinction modeling in various galaxy directions

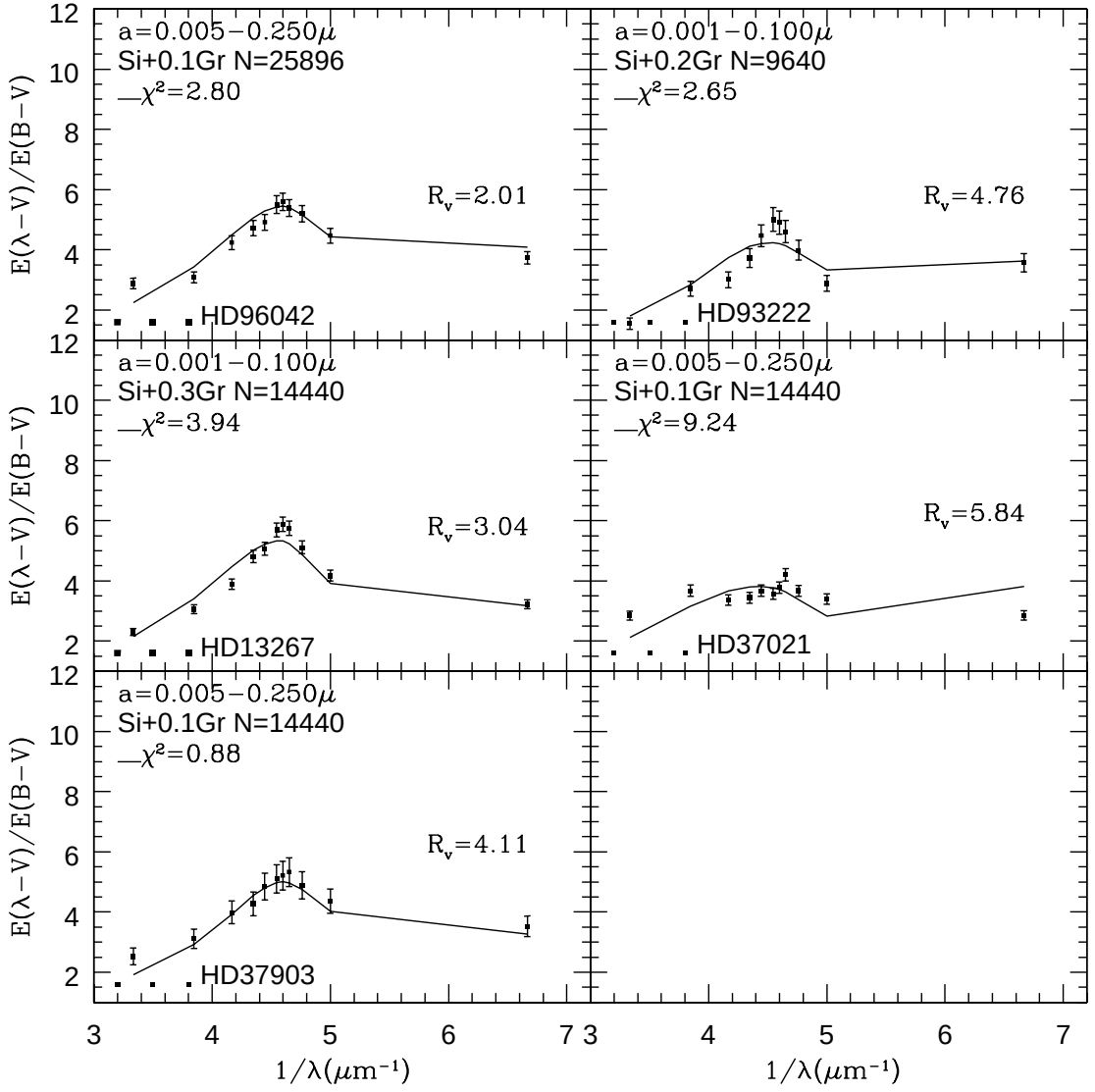

Conclusions & Future Outlook

- We have demonstrated that Spheroidal Composite Grain models can explain the observed interstellar extinction curve, the observed linear polarization curve and also provides a lower estimates for the Carbon abundance which brings closer to the observed ISM values.
- Several workers have recently reported that porous and spheroidal composite dust grains of the type proposed in our models may be the best option for explaining the above observed parameters:

Future Outlook .. contd.

Padoan et. al., ApJ, 649, 807 (2006)
Perets & Biham, MNRAS, 365, 801 (2006)
Stark et. al., A&A, 457, 365 (2006)
Pelkonen et. al., A&A, 461, 551 (2007)
Iati et. al. MNRAS, 384, 591 (2008)

- We are have also attempted to compute the IR emission with the spheroidal composite dust model to explain the IRAS observations as well as the COBE data on diffuse IR emission (Dwek, ApJ, 484, 779, 1997). This will further constrain the Interstellar Dust models (Zubko et. al., ApJS, 152, 211, 2004)

Future Outlook .. contd.

- Upcoming dedicated space missions (ASTROSAT-UVIT and GAIA) will bring out large data base of extinction measurements in many directions of the galaxy and would help in the study of dust distribution within the galaxy by fitting these measurements with Spheroidal Composite dust models. (Bora et al. MNRAS, 384, 827, 2008 – using simulated data for expected output of TAUVEX/ASTROSAT bands – obtain interstellar extinction and Bora et al. New Astronomy, 14, 649, 2009)

Extinction Estimate

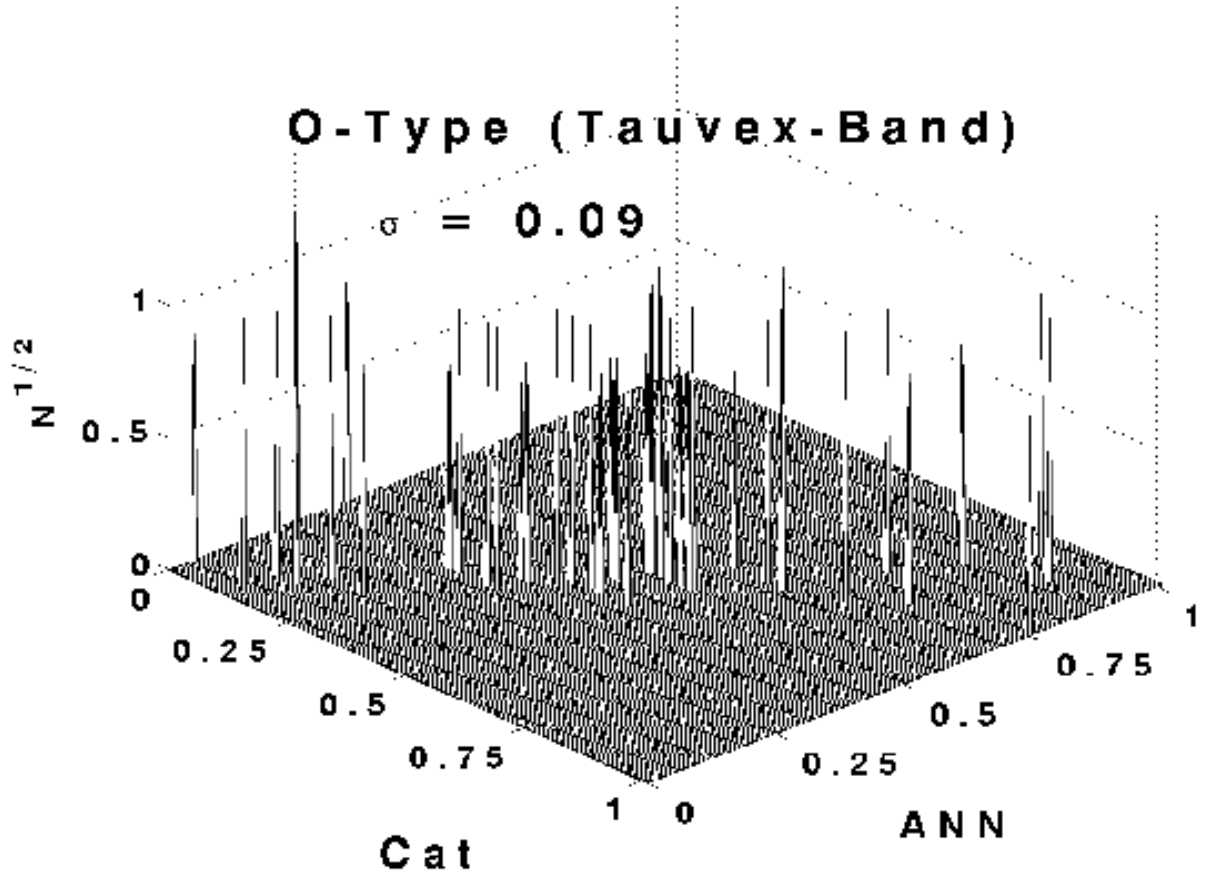

Future Outlook .. contd.

- X-ray scattering is a powerful toll for measuring the size distribution and composition of interstellar dust. Smith & Dwek 1998 (ApJ, 503, 831) have studied the soft X-ray scattering of dust halos around Nova Cygni 1992 using Mie theory, but have mentioned that DDA can be used for this study since 1keV photon has only $\lambda = 1.24$ Å which is substantially smaller than the radius of any grain.

Future Outlook .. contd.

Thus X-ray scattering will be affected by the grain's exact morphology. X-ray observations from ASTROSAT for similar objects and corresponding modeling efforts using composite DDA grains in the X-ray region can provide better insight for understanding the dust behaviour.

Dark Star Forming Clouds CB3

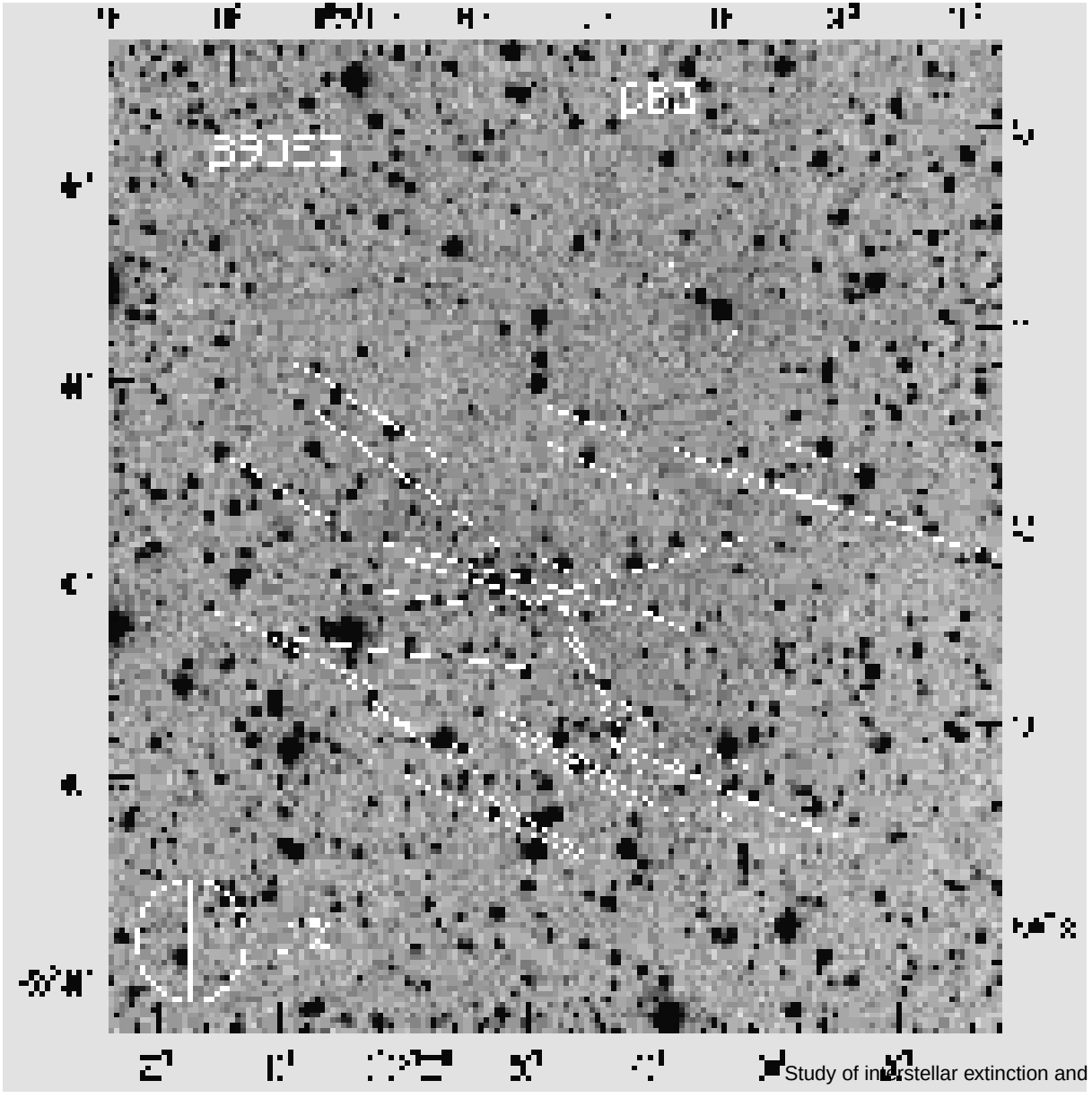

Dark Star Forming Clouds CB25

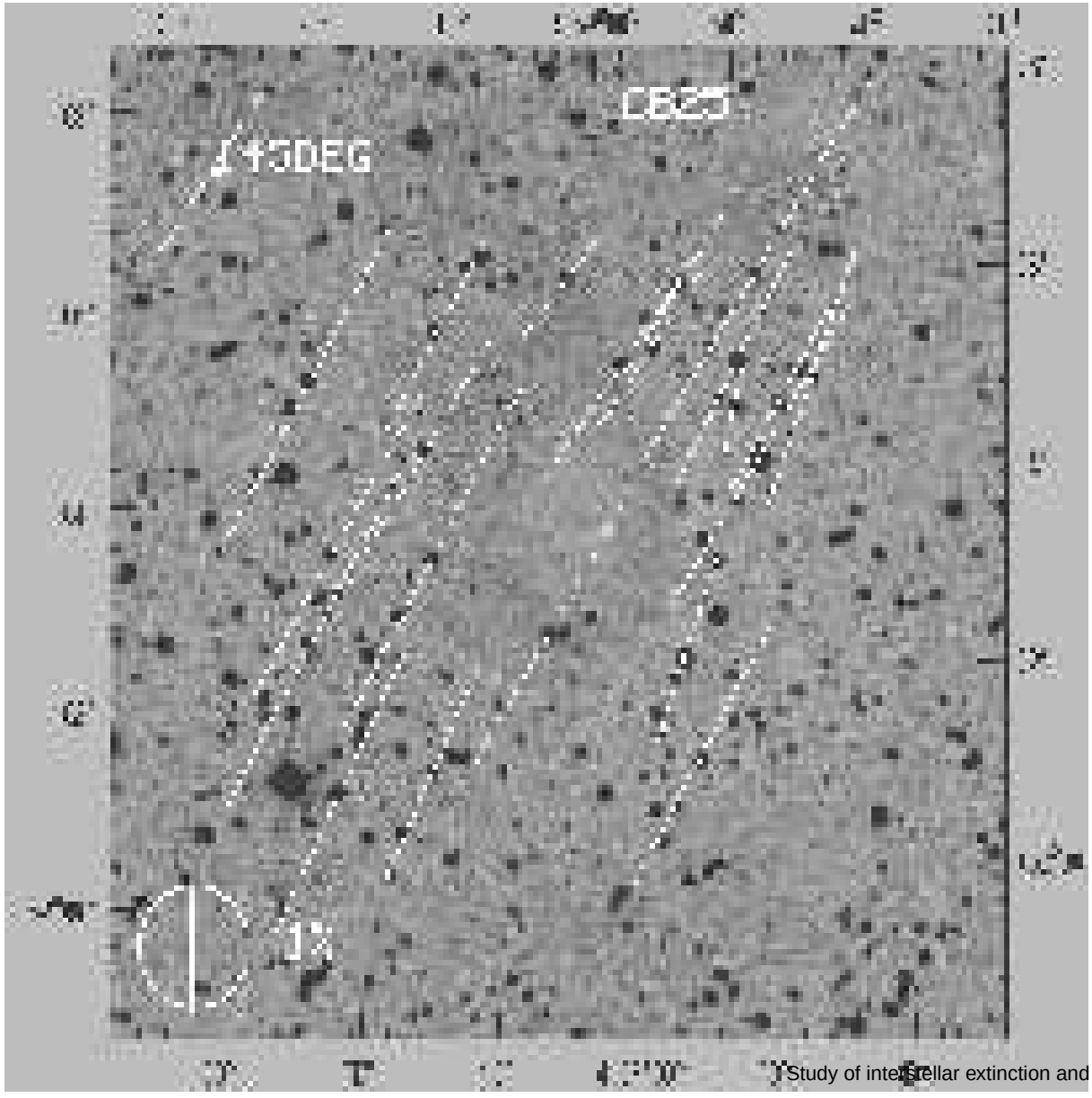

Dark Star Forming Clouds CB39

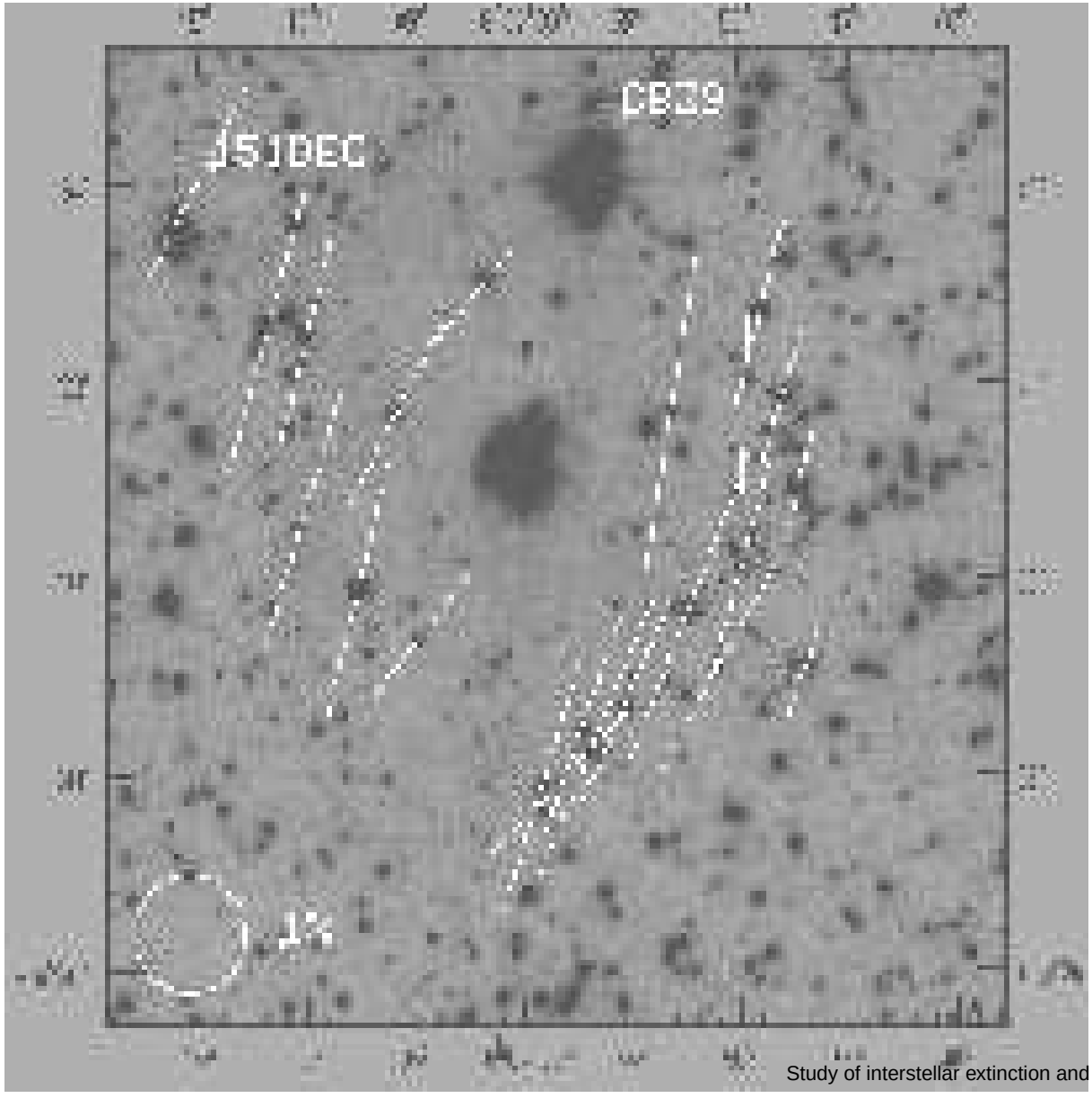

Normal BVR Photometry

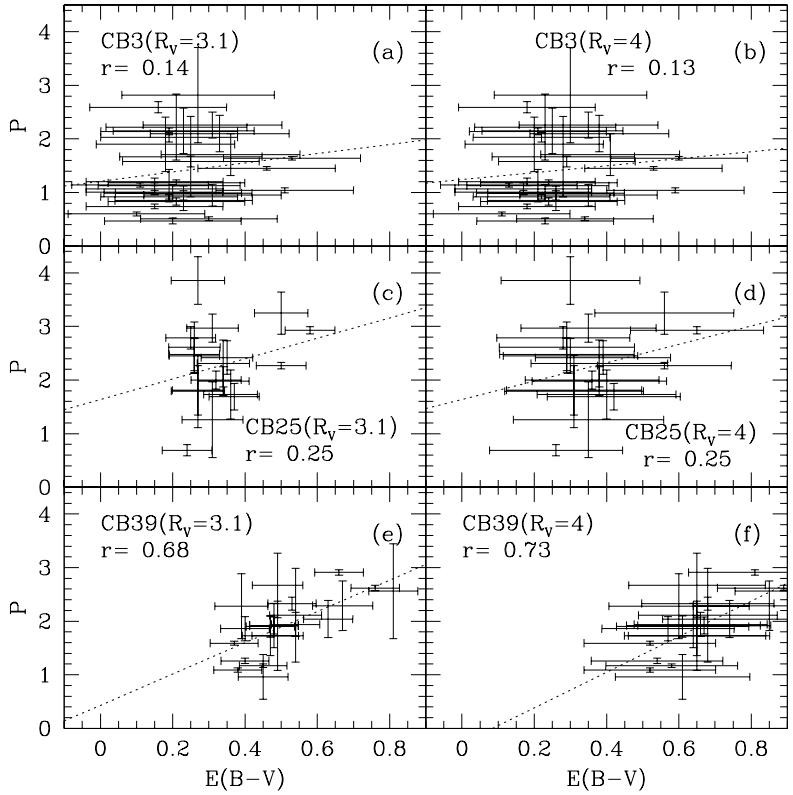

Correlation of Polarization v/s Extinction

Strömgren Photometry

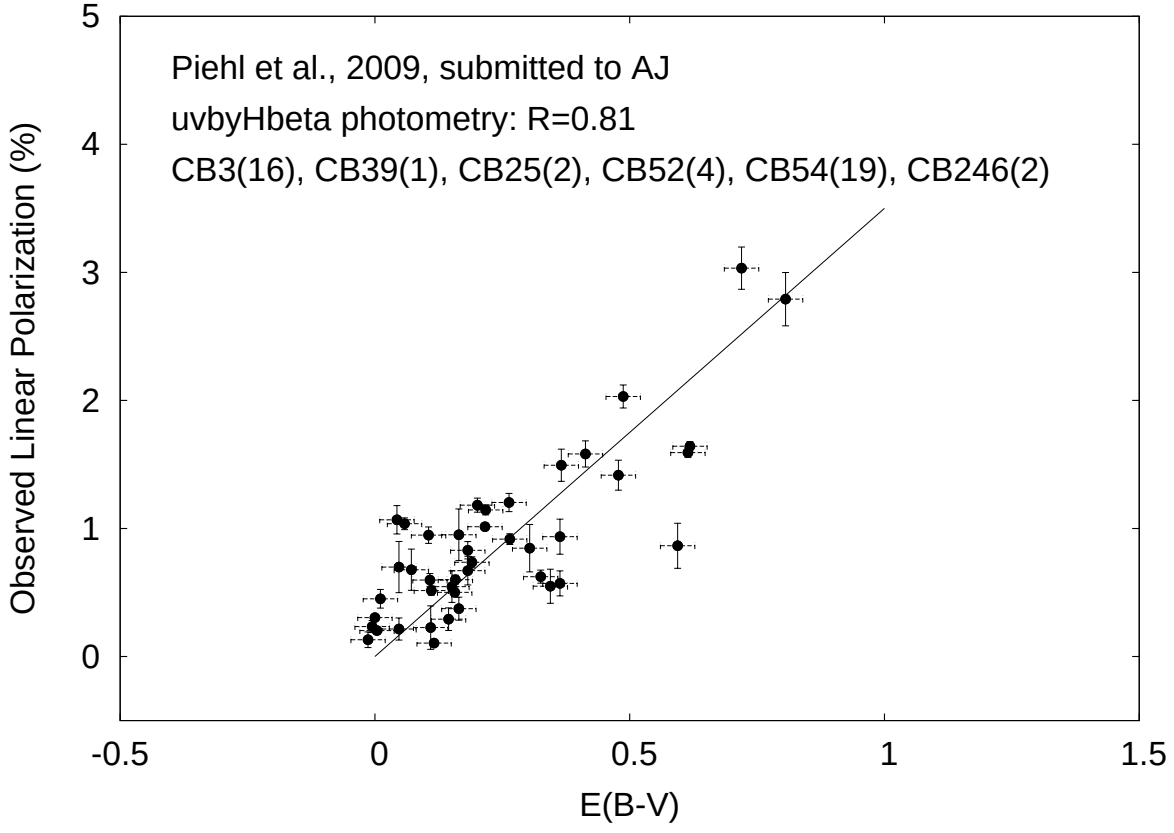

Correlation of Polarization v/s Extinction

Thanks!